2014

EXPERIMENTAL STUDIES ON THE DETERMINATION OF ACOUSTIC BULK MATERIAL PROPERTIES AND TRANSFER IMPEDANCE

Wanlu Li
University of Kentucky, liwanlu10@gmail.com

STUDENT AGREEMENT:

I represent that my thesis or dissertation and abstract are my original work. Proper attribution has been given to all outside sources. I understand that I am solely responsible for obtaining any needed copyright permissions. I have obtained needed written permission statement(s) from the owner(s) of each third-party copyrighted matter to be included in my work, allowing electronic distribution (if such use is not permitted by the fair use doctrine) which will be submitted to UKnowledge as Additional File.

I hereby grant to The University of Kentucky and its agents the irrevocable, non-exclusive, and royalty-free license to archive and make accessible my work in whole or in part in all forms of media, now or hereafter known. I agree that the document mentioned above may be made available immediately for worldwide access unless an embargo applies.

I retain all other ownership rights to the copyright of my work. I also retain the right to use in future works (such as articles or books) all or part of my work. I understand that I am free to register the copyright to my work.

REVIEW, APPROVAL AND ACCEPTANCE

The document mentioned above has been reviewed and accepted by the student's advisor, on behalf of the advisory committee, and by the Director of Graduate Studies (DGS), on behalf of the program; we verify that this is the final, approved version of the student's thesis including all changes required by the advisory committee. The undersigned agree to abide by the statements above.

Wanlu Li, Student

Dr. David W. Herrin, Major Professor

Dr. James McDonough, Director of Graduate Studies

EXPERIMENTAL STUDIES ON THE DETERMINATION OF ACOUSTIC BULK MATERIAL PROPERTIES AND TRANSFER IMPEDANCE

THESIS

A thesis submitted in partial fulfillment of the
requirements for the degree of Master of Science
in Mechanical Engineering in the College of Engineering
at the University of Kentucky

By

Wanlu Li

Lexington, Kentucky

Director: Dr. David W. Herrin, Professor of Mechanical Engineering

Lexington, Kentucky

2014

ABSTRACT OF THESIS

EXPERIMENTAL STUDIES ON THE DETERMINATION OF ACOUSTIC BULK MATERIAL PROPERTIES AND TRANSFER IMPEDANCE

Soft trim absorbing parts (i.e., headliners, backwalls, side panels, etc.) are normally comprised of different layers including films, adhesives, foams and fibers. Several approaches to determine the complex wavenumber and characteristic impedance for porous sound absorbing materials are surveyed and the advantages and disadvantages of each approach are discussed. It is concluded that the recently documented three-point method produces the smoothest results. It is also shown that measurement of the flow resistance and the use of empirical equations is sufficient for many common materials. Following this, the transfer impedance of covers, adhesives, and densified layers are measured using an impedance difference approach. The transfer matrix method was then used to predict the sound absorption of a multi-layered materal which included a perforated cover, fiber layers, and an adhesive. The predicted results agree well with measurement.

KEYWORDS: Sound Absorbing Materials, Sample Variation, Bulk Properties, Covers and Adhesives, Transfer Impedance

Wanlu Li
Student's Signature

18th December, 2014
Date

EXPERIMENTAL STUDIES ON THE DETERMINATION OF ACOUSTIC BULK MATERIAL PROPERTIES AND TRANSFER IMPEDANCE

By

Wanlu Li

Dr. David W. Herrin
Director of Thesis

18th December, 2014
Date

ACKNOWLEDGEMENTS

Foremost, I would like to express my sincere gratitude to my advisor Professor David Herrin for the continuous help of my graduate study and research, for his patience, motivation, enthusiasm, and immense knowledge. His guidance helped me in all the time of research and writing of this thesis. Besides my advisor, I am also grateful to Professor Tingwen Wu, for his encouragement and great help on my research work.

I would also like to thank Professor Tianxiang Li for being my committee member and providing valuable suggestions.

My sincere appreciation also goes to James Haylett, for offering me the summer internship opportunities in CVG and leading me working on diverse exciting projects.

I thank my fellow labmates and friends in Vibro-Acoustics group: Huangxin Chen, Keyu Chen, Gong Cheng, Rui He, Xin Hua, Quentin Hunsucker, Jiazhu Li, Jundong Li, Jiawei Liu, Weiyun Liu, Srinivasan Ramalingam, Kangping Ruan, Shishuo Sun, Peng Wang, Weichen Wang, Robert Wick, Ruimeng Wu, Yitian Zhang, Limin Zhou and Wentao Zhuo, for all the fun we have had in the past several years.

Last but not the least, I would like to thank my parents, for giving birth to me at the first place and supporting me spiritually throughout my life.

.

TABLE OF CONTENTS

LIST OF FIGURES

CHAPTER 1 INTRODUCTION

1.1 Background

Sound absorbing materials are widely used to reduce sound levels in industry. The two most common classes of materials are foams and fibers. Sound is “absorbed” by converting sound energy to heat within the material, resulting in a reduction of the sound pressure. There are two primary mechanisms for achieving this reduction in sound pressure level. One is via vibration of the material skeleton where material damping converts sound to heat. This mechanism is important at low frequencies but is normally small. The far more important mechanism is viscous friction of the fluid (i.e., air) on the material skeleton. Fluid particles oscillate and rub against the material matrix producing heat (Fahy, 2001).

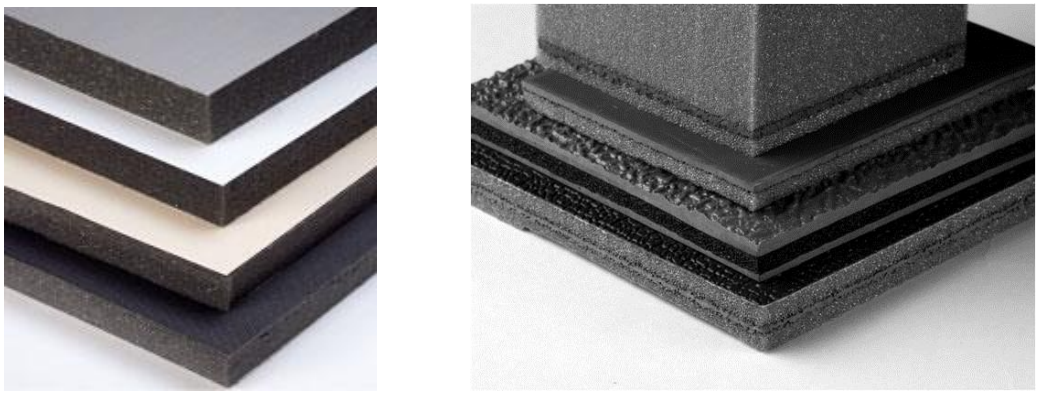

Figure 1.1 Layered sound absorbing materials.

When developing materials, material manufacturers prefer to know the bulk properties (characteristic impedance and complex wave number) instead of the specific boundary impedance or sound absorption. There are several reasons why. First, the sound absorption performance of a material can be determined as a function of the thickness of the sample. Second, models can simulate materials that are stacked or layered (as shown in Figure 1.1) once the bulk properties are known. Additionally, bulk properties can be used directly in finite element analysis and boundary element analysis models. In that case, Jiang and Wu (Jiang and

Wu, 2010) found that the local reacting approximation is not appropriate for materials with lower flow resistivity or for thick sound linings.

Soft trim absorbing parts (i.e., headliners, backwalls, side panels, etc.) are normally comprised of different layers including films, adhesives, foams and fibers. Fiber or foam layers are often fused to one another or a facing using an adhesive or glue (as shown in Figure 1.2 (a)). These layers are often pressed or glued together. Often, a scrim or film facing is used as a cover which adds mass improving the low frequency sound absorption (as shown in Figure 1.2(b)). Recently, a number of suppliers have densified one side of the material so that it performs acoustically similar to a facing. Depending on the process, the densified layer can be permeable or impermeable and is generally lightweight.

Figure 1.2 Sound absorbing materials with (a) adhesive (b) cover.

1.2 Overview

The overall objective of this work is to develop a method for simulating layered sound absorbing materials which include covers and adhesives. In this work, compression of the foam or fiber itself is not included. In the first part of this thesis, the procedure for measuring the normal incident impedance and sound absorption is reviewed. The standards which describe the measurement are ASTM E1050 (1998) or the similar ISO 10534-2 (1998). Though the measurement is commonly performed in academia and industry, users of

impedance tubes know that sample fit has a significant impact on the quality of the measurement. Measurement uncertainty is investigated and recommendations for reducing the uncertainty are summarized. The knowledge gained was used to establish best practices for the measurements that followed.

Designers of acoustic materials commonly use the acoustic wave number and characteristic impedance of the material to predict the performance if the sound absorber thickness is changed or if it is combined with other materials in a layered absorber. There are a number of different ways to determine these bulk properties using an impedance tube. There are two main classes of measurement approaches. The first class is to directly measure the bulk properties using either the two-load, two-cavity, or three-point approaches with an impedance tube. The second is to measure the flow resistivity or the sound absorption and estimate the bulk properties from empirical or analytical equations. Each of these methods are surveyed and recommendations are made.

Thin layers like perforates, foil covers, adhesives, or densified layers are normally modeled as a transfer impedance. The transfer impedance is commonly measured using an impedance difference approach (Wu et al, 1988). In prior research, the impedance difference approach has been used to determine the transfer impedance of rigid perforated materials. In this thesis, the approach is extended and applied to the measurement of adhesives and densified layers.

The aforementioned procedures were then validated for a multi-layer sound absorber which included a perforated cover, and separate layers of fiber and foam bonded together by an adhesive. The transfer impedances of the cover and adhesive were measured using the impedance difference approach. The bulk properties of the fiber and foam were measured using the three-point method. The transfer matrix approach was then used to predict the sound

absorption of the layered sound absorber. The predicted results agreed well with measurement.

1.3 Organization

This thesis contains eight chapters which can be divided into four main parts:

Chapter 2 examines the uncertainty in impedance tube measurements to determine the sound absorption using ASTM E1050. Several ways to reduce measurement uncertainty are also discussed in this chapter.

Chapter 3 and Chapter 4 survey the different methods for determining the bulk properties of fibers and foams. Chapter 3 details the procedures and equations used and chapter 4 compares results between the methods.

Chapter 5 and Chapter 6 detail the impedance difference approach to determine the transfer impedance of glues and covers. Chapter 5 illustrates the effect of glues, covers, and material compression on the sound absorption. The impedance difference approach is also detailed and validated. Chapter 6 shows transfer impedance results for glues and covers. In addition, an empirical model is used to predict the transfer impedance for a commercially available adhesive.

In Chapter 7, the sound absorption of a layered absorber is predicted using the transfer matrix approach and validated via measurement. Results show good agreement and demonstrate that the approaches documented can be used to predict the performance of a layered material. Results suggest that complicated layered materials including adhesives and covers can be designed.

Chapter 8 concludes the thesis by summarizing the major findings, the contribution made, and includes some recommendations for future work.

CHAPTER 2 EFFECT OF SAMPLE VARIATION

2.1 Sample Variation

The most useful metric for assessing the effectiveness of a sound absorbing material is the normal incident sound absorption coefficient. It is defined as the ratio of the absorbed to incident sound power. The metric assesses the effectiveness of the material and is a repeatable and relatively inexpensive test. This measurement procedure has been standardized in ASTM E1050 (1998). A typical apparatus is shown in Figure 2.1. A loudspeaker placed on one end of an impedance tube is used to generate sound and a cylindrical sample is placed at the other end of the tube. The transfer function between the two microphones is measured and the reflection coefficient (R) can be determined.

$$R = \frac{H_{12} - e^{-jks}}{e^{jks} - H_{12}} e^{2jkx_1} \tag{2.1}$$

where k is the wave number ($2\pi f/c$) where *f* is the frequency in Hertz and c is the speed of sound. The normalized surface impedance of the sample can be calculated from the reflection coefficient (R) and is expressed as:

$$z = \frac{Z}{\rho c} = \frac{1 + R}{1 - R} \tag{2.2}$$

where $\boldsymbol{\rho}$ is the air density. The normal incident sound absorption (α) is expressed as

$$\alpha = 1 - |R|^2 \tag{2.2}$$

The impedance tube used for the measurements that follow is a Spectronics 1.375 inch diameter tube equipped with PCB ½ inch ICP microphones (377B11) and a JBL 70W compression driver (JBL 2426H).

Samples were cut using a cylindrical steel blade in a drill press. Care was taken to avoid hourglassing or deforming the sample.

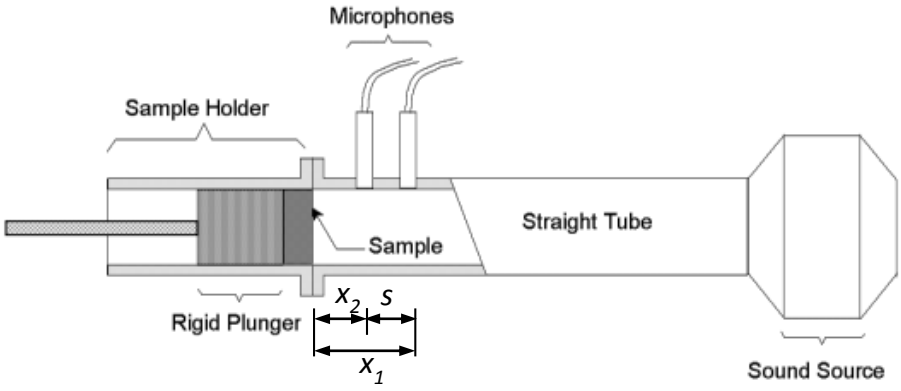

Figure 2.1 Schematic diagram of two microphone method apparatus.

Despite proper care, there will be variations between measurements due to sample variation and the measurement procedure itself. Foams are manufactured by mixing chemicals at high temperature until the foam rises in a process similar to baking. The foam often is not homogeneous. In addition, there are often variations from batch to batch. Accordingly, variation in the normal impedance and sound absorption is expected. Glass fiber manufacturing is the high-temperature conversion of various raw materials into a homogeneous melt, followed by the fabrication of this melt into glass fibers (Office of Air Planning and Standards, 1995). Glass fiber has less sample variation than foam due to the manufacturing procedure.

In addition, the measurement procedure itself can lead to variability. Several factors can contribute. These include:

1. Sample size. Considerable care should be taken when preparing the material sample for measurement. The sample should fit snugly but not be compressed in the tube (Seybert, 2013, Hua, 2013, Stanley, 2012). If the sample is cut too small, there will be gaps between the sample and the tube

which will lead to poor results. If the sample is compressed, additional structural resonances of the solid frame are introduced.

2. Sample shape. The sample geometry should be that of a uniform concentric cylinder. Hourglassing of the sample can occur if the sample is not carefully cut or if the cutting procedure is faulty (Stanley, 2012).
3. Sample mounting. The sample should be mounted so that it is flush against the back of the holder.

Stanley provided some suggestions in sound absorption coefficient measurement (Stanley, 2012) and they are summarized as followed (Seybert, 2013, Hua, 2013):

1. Start with material sheets of uniform thickness without warps and free of dirt and moisture.
2. Material sheets that meet the above criteria must meet chemical and physical specifications of the manufacturer.
3. The best samples are cut using a waterjet cutter, but rotating blade cutters may also be used.
4. Cut at least three and preferably five samples for testing to obtain a good average.
5. Samples should be right, circular cylinders – no bulges, cups, and without inclination.
6. Mark and test the same side of all samples.
7. Sample fit in the sample holder is critical. When the sample holder is held vertically, the sample should remain in the sample holder but only barely.
8. Facings must not extend beyond the diameter of the sample – careful trimming may be needed.

The remainder of this chapter examines the measurement variation in glass fiber and melamine foam.

2.1.1 Variability of Melamine Foam

6 Samples of 0.5 inch and 0.75 inch thick 0.6 lbs/ft³ melamine foam were measured in an impedance tube according to ASTM E1050. All the samples are cut from the same sheet of foam. Figures 2.2 and 2.3 show the sound absorption for 6 samples of 0.5 inch and 0.75 inch thick melamine foam respectively. Figure 2.4 shows the standard deviation of the sound absorption coefficient for 6 samples each of 0.5 inch and 0.75 inch melamine foam. Most variation occurs between 3000 to 4000 Hz for 0.5 inch samples and 2500 to 3000 Hz for 0.75 inch samples. These variations are likely due to shearing resonances of the sample due to the edge constraints (Song and Bolton, 2001).

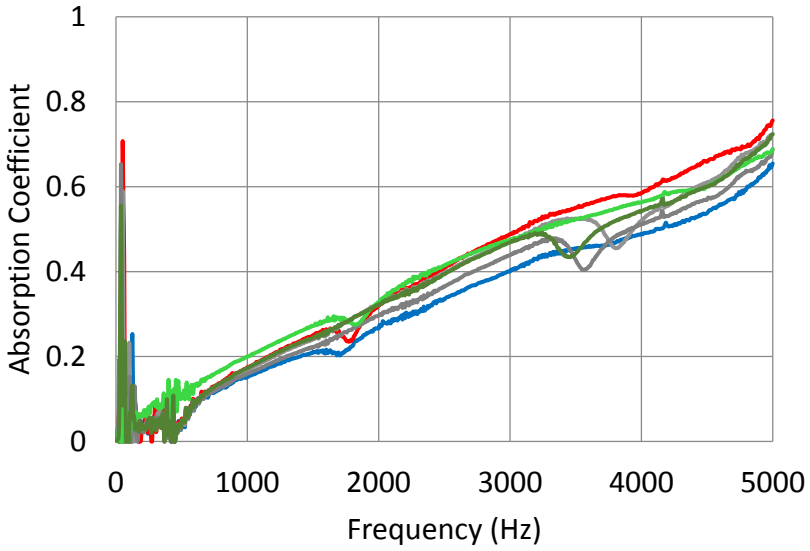

Figure 2.2 Sound absorption coefficient of 6 samples of 0.5 inch 0.6 lbs/ft³ melamine.

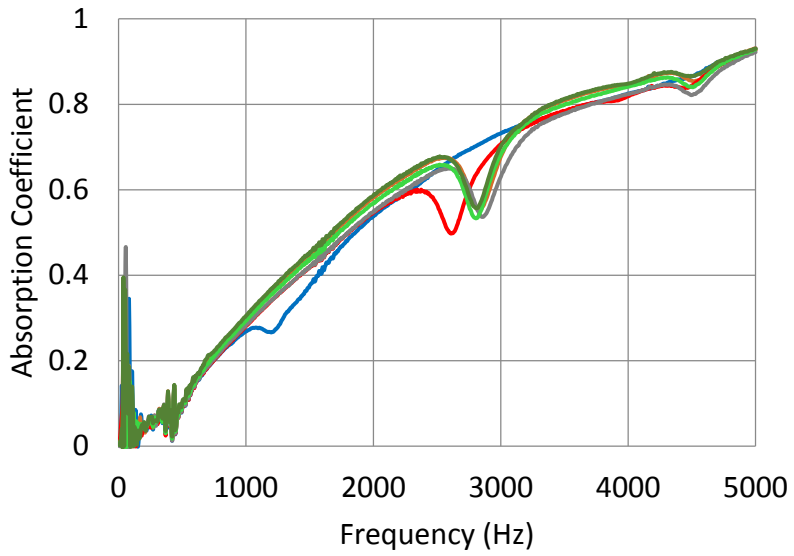

Figure 2.3 Sound absorption coefficient of 6 samples of 0.75 inch 0.6 lbs/ft³ melamine.

There is also significant variation below 500Hz. The sound source is a compression driver loudspeaker that has insufficient strength at lower frequencies. In addition, the sound absorption coefficient is very low and sound absorption in the tube itself will lead to inaccuracies (Seybert, 2013, Hua, 2013). An example using a high power compression driver is shown in Section 2.2.1.

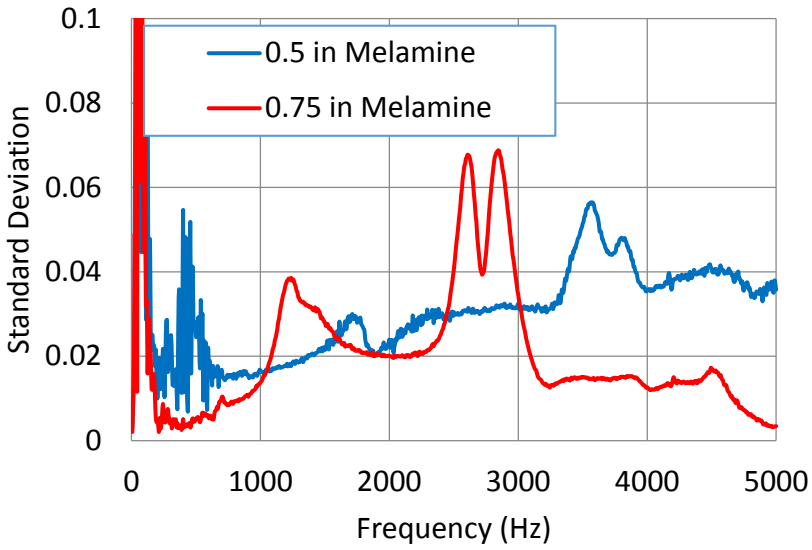

Figure 2.4 Standard deviation of 6 samples of 0.5 and 0.75 inch melamine foam.

2.1.2 Variability of Glass Fiber

8 samples of 2 inch glass fiber are measured and the sound absorption coefficient is shown in Figure 2.5. The variability is much lower in the case of a glass fiber. The reason is primarily due to the cutting. Fiber does not hourglass as much as foam and it will not deform the entire sample even if the fit in the impedance tube is a little too snug.

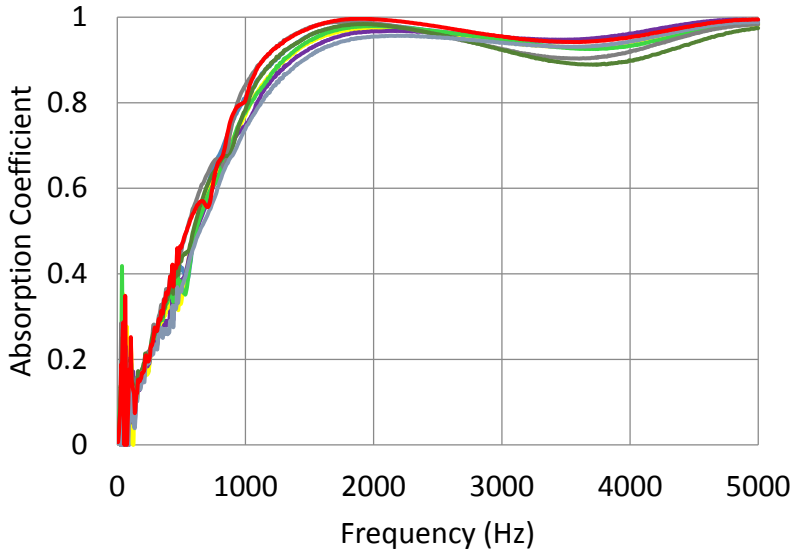

Figure 2.5 Sound absorption coefficient of 8 samples of 2 inch fiber.

Figure 2.6 shows the standard deviation of 8 samples of 2 inch glass fiber. Larger deviations occur under 800 Hz due to shear resonances of the elastic frame that are inconsistent between samples.

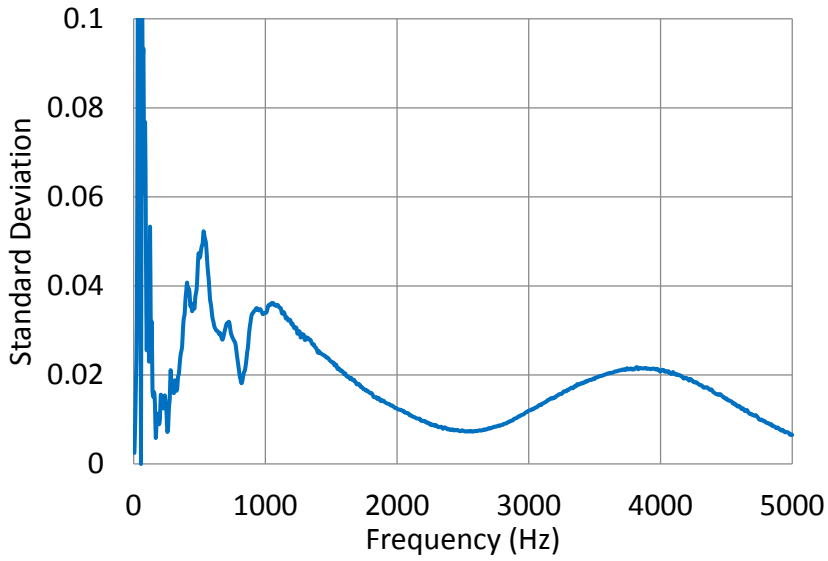

Figure 2.6 Sound absorption coefficient standard deviation for 8 samples of 2 inch fiber.

2.1.3 Effect of Impedance Tube Size

8 Samples of 2 inch fiber glass are measured in both 1.370 inch and 3.875 inch diameter impedance tube. The averaged absorption coefficient of 8 samples for each size of impedance tube is shown in Figure 2.7. The average sound absorption coeffcient measured by both 1.370 and 3.875 inch tubes compare well except at frequencies below 500 Hz.

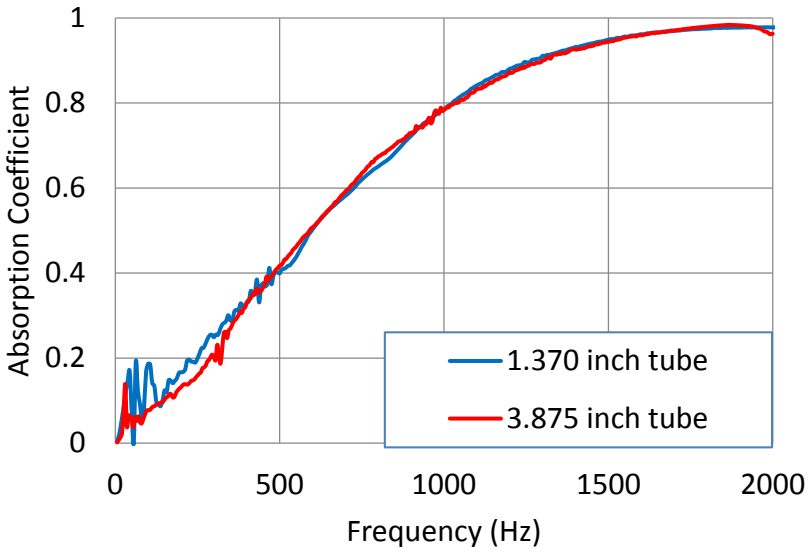

Figure 2.7 Effect of impedance tube size on 8 samples of 2 inch fiber.

Figure 2.8 shows the sound absorption coefficient standard deviation for 8 samples of 2 inch fiber measured in both 1.370 and 3.875 inch impedance tubes. The standard deviation is slightly lower for the larger impedance tube. There are several likely reasons. First, all the samples are cut by rotating blade cutters. The cutter size for the 1.370 inch diameter tube is 0.005 inch larger while the cutter size for the 3.875 inch tube is the same with the size of the tube. The sample size should not exceed the size of the impedance tube to avoid adding additional edge constraints on the frame of the material (Song and Bolton, 2001). Details about the effect of sample size are covered in Section 2.2. In addition, edge effects are more important in a smaller tube since the perimeter to cross-sectional area ratio is higher. Morever, The sound source used in the 3.875 inch impedance tube has higher sound power at low frequencies than that used in the small impedance tube. This will reduce the measurement variability at low frequencies (Seybert, 2013, Hua, 2013).

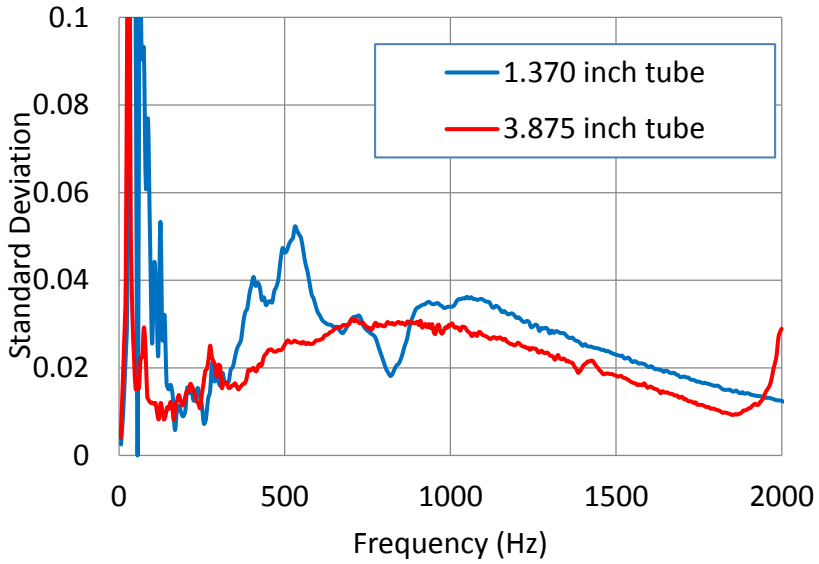

Figure 2.8 Standard deviation of 8 samples of 2 inch fiber in 1.370 and 3.875 inch impedance tubes.

2.2 Minimizing Sample Variation

The measurement variation can be controlled by carefully preparing the samples and using an adequate source.

2.2.1 Sample Preparation

8 samples of 1 inch thick 0.6 lbs/ft³ Melamine were cut using 1.375 inch and 1.360 inch diameter cutters, respectively, and measured using the 1.370 inch diameter impedance tube. The averaged sound absorotion coefficient of two sets of foam samples is shown in Figure 2.9. Both of the results compare well except at the shear resonance in the 1.375 samples. This resonance occurs because the sample is oversized and consequently compressed..

Samples should be cut to match or be slightly smaller than the size of the impedance tube. A grinding machine or sandpaper can be used to trim the edge of oversized samples. One can also use vaseline to seal the small gaps between the sample and the tube wall to increase the accuracy.

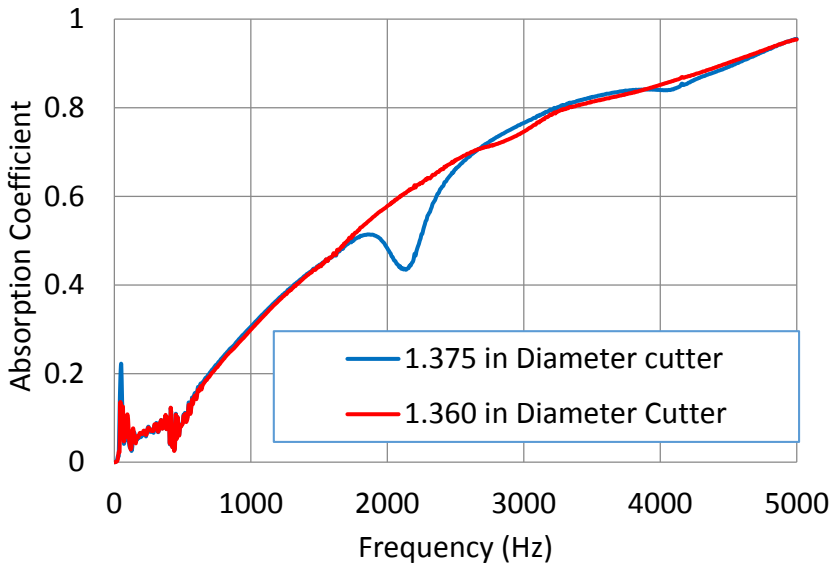

Figure 2.9 Effect of cuter size on 8 samples of 1 inch 0.6 lbs/ft³ melamine foam.

4 Samples of 0.5 inch 0.6 lbs/ft³ Melamine foam cut by the 1.375 inch cutter were filed using sandpaper and measured using the 1.370 inch diameter impedance tube. The unfiled sample measurement result was shown in Figure 2.2. Figure 2.10 shows the absorption coefficient result for the filed samples. Note that a higher power loudspeaker (JBL 2447H, 100W) was used in place of the original (JBL 2426H, 70W). The standard deviations for both filed and unfiled samples are shown in Figure 2.11. The standard deviation is greatly reduced over the entire frequency range. This is especially the case for the resonance frequencies around 500 and 3500 Hz.

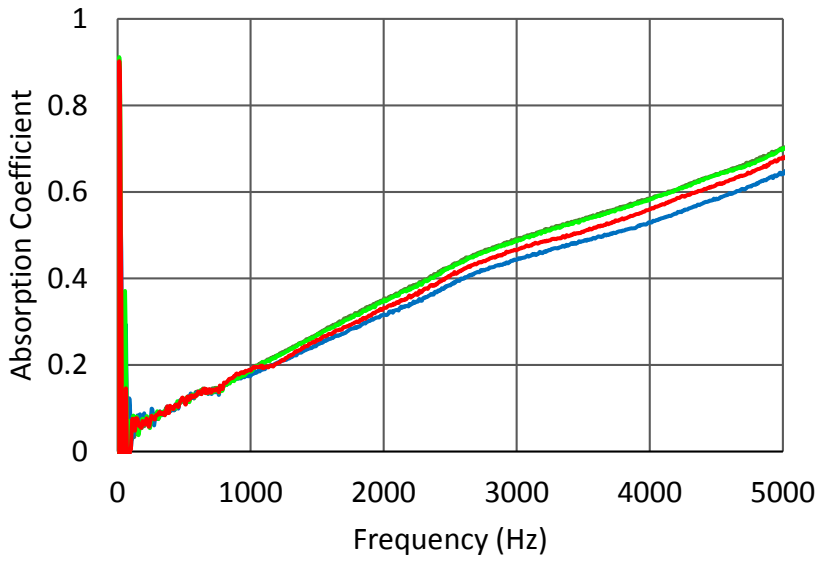

Figure 2.10 Variability of 4 samples of 0.5 inch 0.6 lbs/ft³ melamine.

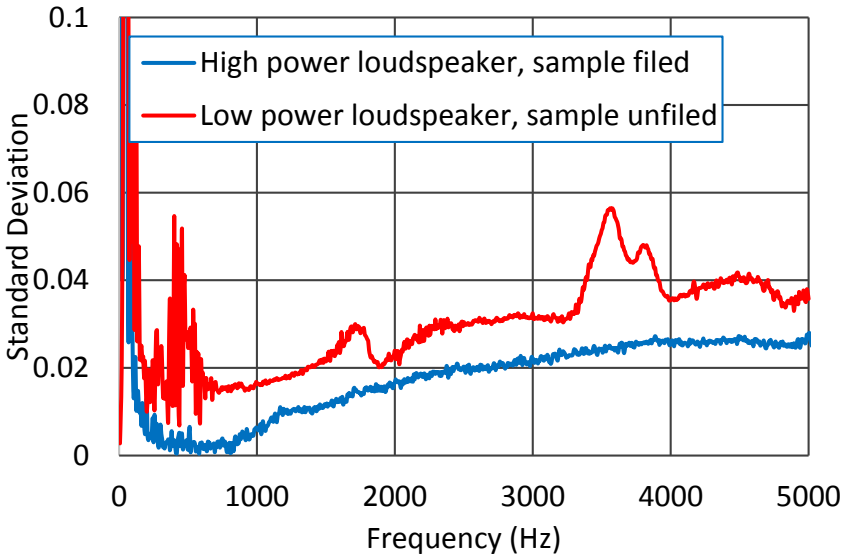

Figure 2.11 Standard deviation comparison of 0.5 inch 0.6 lbs/ft³ melamine.

2.2.2 Adding Needles in Samples

If the sample diameter is greater than the tube diameter, shear resonances may occur and the accuracy will be reduced. There is an alternative way to treat oversized samples in order to minimize sample variation. Adding needles in

samples appears to minimize the resonant behavior of the sample (ESI Group, 2010).

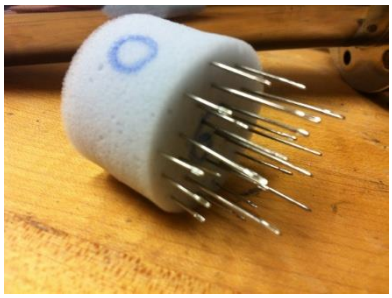

Figure 2.12 Adding needles in 1 inch 0.6 lbs/ft³ melamine.

Figure 2.12 shows a photograph where 25 needles were added to a sample of 1 inch thick melamine foam. Adding needles in a material appears to constrain the motion of its elastic frame. As shown in Figure 2.13, resonance behavior moves to higher frequencies by increasing the number of needles in the sample. Adding 25 needles increases the resonance frequency outside the frequency range of interest.

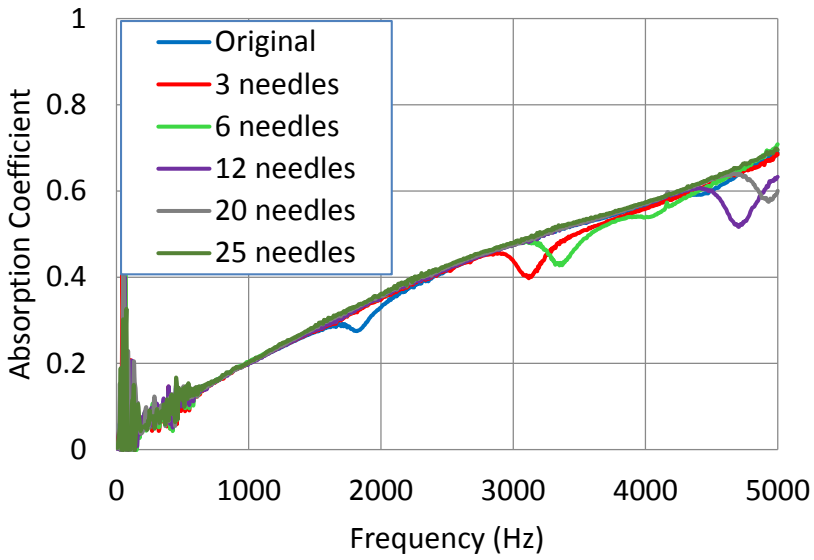

Figure 2.13 Effect of adding needles on 0.5 inch 0.6 lbs/ft³ melamine foam.

Figure 2.14 compares the sound absorption coefficient of the oversized sample with and without needles. Note that the sound absorption in the sample is not affected greatly by adding needles.

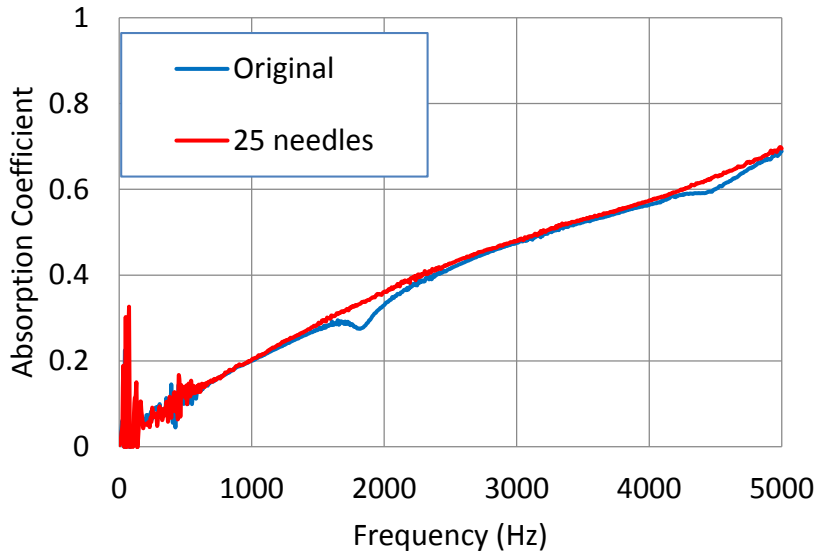

Figure 2.14 Effect of adding 25 needles on 0.5 inch 0.6 lbs/ft³ melamine foam.

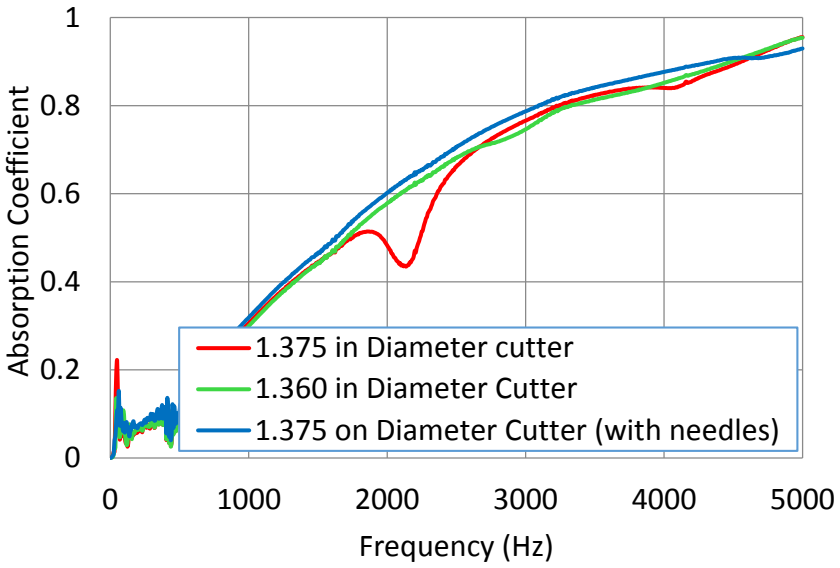

Figure 2.15 Averaged sound absorption coefficient for 8 Samples of 1 inch 0.6 lbs/ft³ melamine foam.

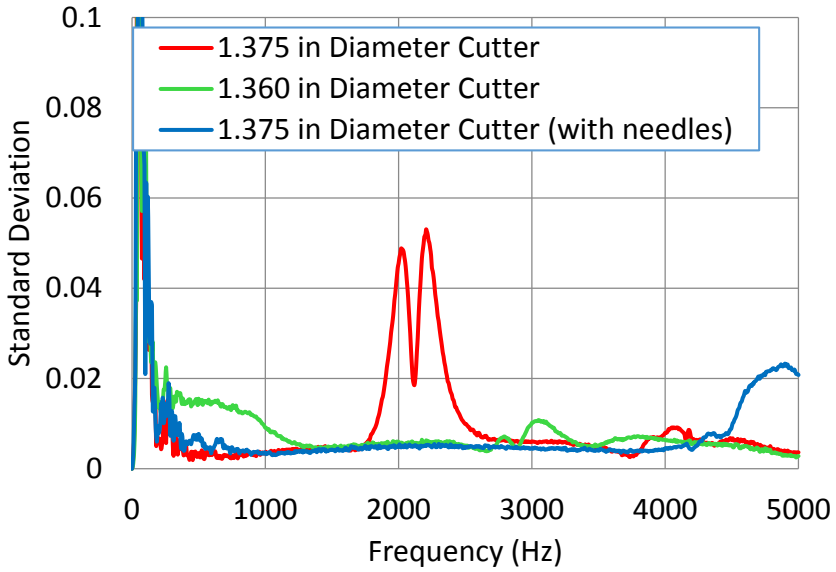

Figure 2.16 Sound absorption coefficient standard deviation of 8 Samples of 1 inch 0.6 lbs/ft³ melamine foam.

Sample variation can be minimized by a proper sample size and adding needles in the material. Figure 2.15 compares the averaged absorption coefficient of three sets of foam samples. One set is 0.005 inch larger than the diameter of the impedance tube, while the other set is slightly smaller than the size of the impedance tube. The third set is oversized but treated by adding 25 needles. 8 samples were used for each set of measurements. The standard deviation is shown in Figure 2.16. Note that the standard deviation can be decreased by either cutting the sample size slightly smaller than the tube or by adding needles.

2.3 Summary

The effect of sample variation was investigated for both melamine foam and glass fiber. Sample variation at high frequencies can be minimized by a proper sample size and adding needles in the sample. Sample variation at low frequencies can be improved by using a higher power sound source.

CHAPTER 3 METHODS FOR MEASURING BULK PROPERTIES

3.1 Introduction

Bulk material properties consist of the complex wavenumber and characteristic impedance, or, alternatively, the complex speed of sound and density. Bulk properties can be measured directly using the two load (ASTM, 2009), two source (Tao, 2003), or two cavity (Utsuno, 1989) methods. Iwase et al. (1998) developed a three microphone method and Salissou and Panneton (Salissou and Panneton, 2010) recently modified the method to use measured transfer functions in the algorithm. Direct measurement of the bulk properties requires an impedance tube, and considerable care should be taken when preparing samples and positioning them.

Alternatively, the bulk properties are often found using indirect means by estimating them from a measurement of the flow resistivity (ASTM 2003) or the sound absorption (Simon, 2006, ESI, 2007). These methods utilize empirical (Delay and Bazley, 1970, Mechel, 1988, Wu, 1988) or theoretical (Allard, 2009) equations.

This chapter will review the many methods (summarized in Figure 3.1) to determine the bulk properties of sound absorbing materials. Direct measurement of the bulk properties will be discussed first followed by a look at the approximate methods. The advantages and disadvantages of each approach will be summarized in the next chapter.

Figure 3.1 summarizes the methods that can be used to determine the bulk properties of a sound absorbing material. The bulk properties can be determined by:

1. Direct measurement using an impedance tube.
2. Measuring the flow resistance and inputting the result into empirical equations.

3. Measurement of the sound absorption and curve fitting to determine the flow resistivity or the Biot parameters.

Each of these approaches are examined in detail.

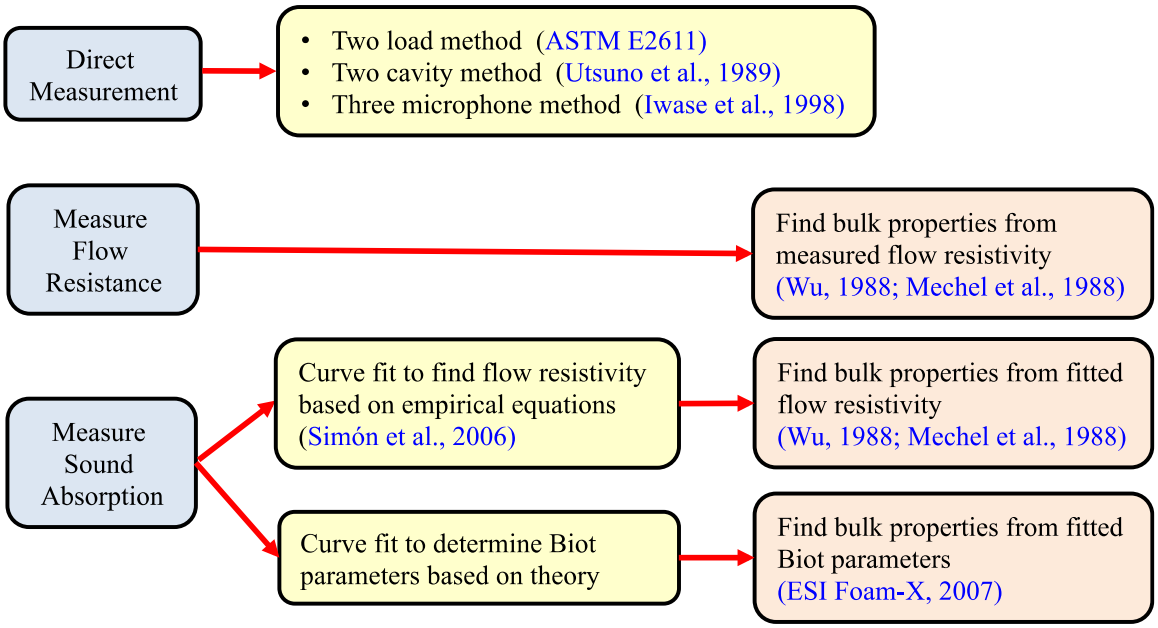

Figure 3.1 Methods for finding bulk sound absorbing properties.

3.2 Direct Measurement Methods

3.2.1 Two-Load Method

In the case of the two-load method, a sample is placed inside the impedance tube. There is a cavity between the sample and the end of the impedance tube and measurements are made with two different acoustic loads. A transfer matrix of the sample can be found using the process outlined as follows.

A schematic illustrating the two-load method is shown in Figure 3.2. Transfer functions are measured between Microphone 1 and the other 3 microphones for each of the two load cases. The acoustic load is most easily modified by changing the termination. ASTM E2611 (ASTM, 2009) details the recommended algorithm

for determining the four-pole matrices and bulk properties for the material. The essentials of the algorithm are presented next.

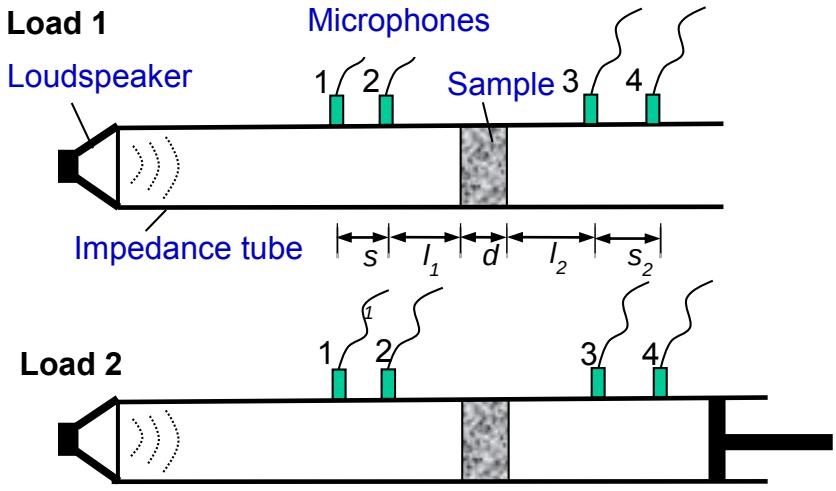

Figure 3.2 Schematic diagram of two load method apparatus.

The transfer matrix, which relates the sound pressure and particle velocity on one side of a sample to that on the other, can be determined in the following manner from the measurements. The incident pressure amplitudes upstream and downstream are expressed as

$$P_A = j\frac{e^{-jkl_1} - H_{21}e^{-jk(l_1+s_1)}}{2\sin ks_1} \quad P_B = j\frac{H_{21}e^{jk(l_1+s_1)} - e^{jkl_1}}{2\sin ks_1}$$
$$P_C = j\frac{H_{31}e^{jk(l_2+s_2)} - H_{41}e^{jkl_2}}{2\sin ks_2} \quad P_D = j\frac{H_{41}e^{-jkl_2} - H_{31}e^{-jk(l_2+s_2)}}{2\sin ks_2} \tag{3.1}$$

where H_{21}, H_{31}, and H_{41} are the respective transfer functions assuming microphone i is used as a reference for phase. l_1, l_2, s_1 and s_2 are dimensions between microphones and the sample as shown in Figure 3.2. The sound pressure and particle velocity at the inlet and outlet to the sample can be expressed as

$$p_1 = P_A + P_B \quad u_1 = (P_A - P_B)/\rho c$$
$$p_2 = P_c e^{-jkd} + P_D e^{jkd} \quad u_2 = \left(P_C e^{-jkd} - P_D e^{jkd}\right)/\rho c \tag{3.2}$$

and then the transfer matrix can be expressed as

$$\begin{Bmatrix} \tilde{p}_1 \\ S_1 \tilde{u}_1 \end{Bmatrix} = \begin{bmatrix} \dfrac{p_{1a}u_{2b} - p_{1b}u_{2a}}{p_{2a}u_{2b} - p_{2b}u_{2a}} & S\dfrac{p_{1b}p_{2a} - p_{1a}p_{2b}}{p_{2a}u_{2b} - p_{2b}u_{2a}} \\ S\dfrac{u_{1a}u_{2b} - u_{1b}u_{2a}}{p_{2a}u_{2b} - p_{2b}u_{2a}} & \dfrac{p_{2a}u_{1b} - p_{2b}u_{1a}}{p_{2a}u_{2b} - p_{2b}u_{2a}} \end{bmatrix} \begin{Bmatrix} \tilde{p}_2 \\ S_2 \tilde{u}_2 \end{Bmatrix} \tag{3.3}$$

where the subscripts a and b indicate the respective loads. The 2×2 matrix in Equation 4 can be related to the complex wavenumber and characteristic impedance as

$$\begin{bmatrix} A & B \\ C & D \end{bmatrix} = \begin{bmatrix} \cos(k_c d) & \dfrac{j}{S}\rho' c' \sin(k_c d) \\ jS\sin(k_c d)/\rho' c' & \cos(k_c d) \end{bmatrix} \tag{3.4}$$

The characteristic impedance and complex wavenumber can then be expressed as

$$z_c = \sqrt{\frac{B}{C}} \tag{3.5}$$

and

$$k_c = \frac{\arctan\left(\dfrac{B}{jAz_c}\right)}{d} \tag{3.6}$$

respectively.

Sometimes the bulk properties are alternatively expressed as a complex speed of sound and density. These quantities are typically used in acoustic simulation software as inputs for boundary and finite element models. In that case, the

complex speed of sound and density can be expressed in terms of the complex wavenumbers and characteristic impedance as

$$c' = \frac{\omega}{k_c} \tag{3.7}$$

and

$$\rho' = \frac{k_c z_c}{\omega} \tag{3.8}$$

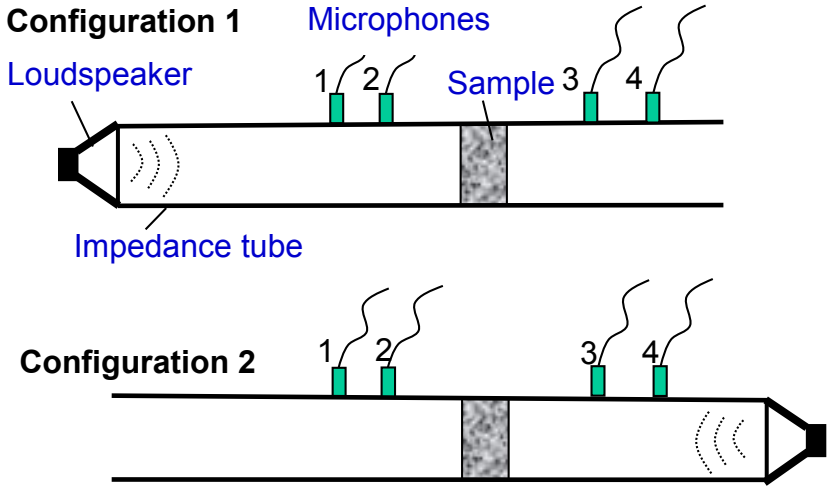

Figure 3.3 Schematic diagram of two source method apparatus.

Though not often used, a similar two-source method (Tao, 2003) can also be used to find the bulk properties. Measurements are made with the source in two configurations. The source is placed on the left end of the impedance tube and then it is placed on the right end of the tube (See Figure 3.3). If the sample is placed symmetrically between the two microphones and the material can be assumed isotropic, the measurement need only be made once. The algorithm is identical to the two-load method except loads a and b now refer to source configurations a and b.

3.2.2. The Two Cavity Method

Alternatively, the bulk properties can be ascertained by measuring the normal incidence impedance for two different cavity lengths (Utsuno,1989) using ASTM E1050. Figure 3.4 shows a schematic of the measurement setup. The primary advantage of this approach is that measurements are not required behind the sample. Normally, there is higher signal to noise for a microphone that is placed between the source and the sample so the measured data should be better-quality.

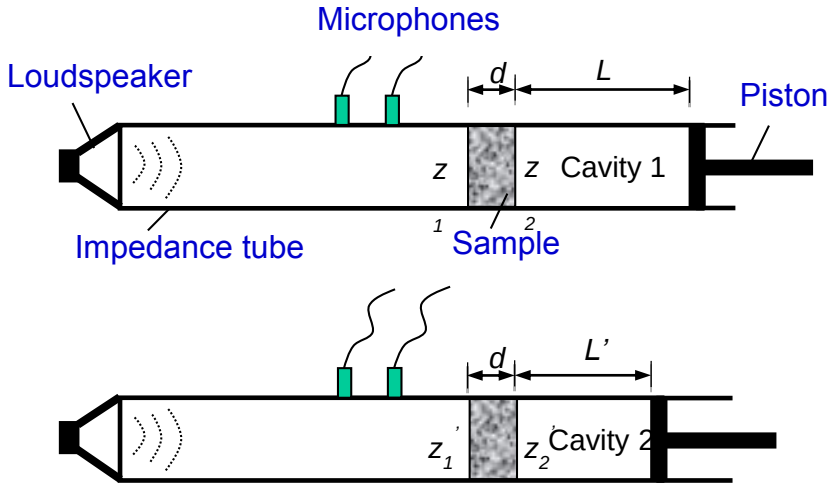

Figure 3.4 Schematic diagram of two cavity method apparatus.

The characteristic impedance can be calculated using

$$z_c = \pm\sqrt{\frac{z_1 z_1'(z_2 - z_2') - z_2 z_2'(z_1 - z_1')}{(z_2 - z_2') - (z_1 - z_1')}} \tag{3.9}$$

Where $z_2 = -j\rho c\cot(kL)$ and $z_2' = -j\rho c\cot(kL')$. The complex wavenumber is determined using

$$k_c = \left(\frac{1}{2jd}\right)\ln\left(\frac{(z_1 + z_c)(z_2 - z_c)}{(z_1 - z_c)(z_2 + z_c)}\right) \tag{3.10}$$

3.2.3. The Modified Three Microphone Method

The three microphone method was originally developed by Iwase et al. (1998) to measure the bulk properties. Salissou and Panneton (2010) improved the method by positioning the microphones upstream and not flush against the sample and used measured transfer functions in the algorithm. The test setup is similar to the two-microphone method (ASTM, 1998) except a third microphone is placed at the rear of the sample as shown in Figure 3.5. The advantage of the method is that a single load is sufficient.

The justification by Salissou and Panneton for the method follows. Sound pressure at any point of the tube can be expressed as:

$$p(x) = Ae^{-jkx} + Be^{jkx} \tag{3.11}$$

It follows that the transfer function between points 1 and 2 can be expressed as:

$$H_{12} = \frac{P(x_2)}{P(x_1)} = \frac{Ae^{jkL} + Be^{-jkL}}{Ae^{jk(s+L)} + Be^{-jk(s+L)}} = \frac{e^{jkL} + Re^{-jkL}}{e^{jk(s+L)} + Re^{-jk(s+L)}} \tag{3.12}$$

Where R is the reflection coefficient.

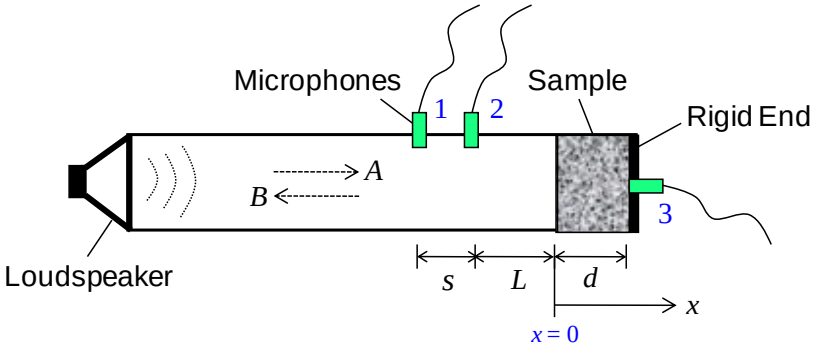

Figure 3.5 Schematic diagram of three microphone method apparatus.

Solving for R :

$$R = \frac{e^{jks} - H_{12}}{H_{12} - e^{-jks}} e^{2jkL} \tag{3.13}$$

And the specific boundary impedance (Z_s) of the sample can be expressed as:

$$Z_s = Z_0 \frac{1+R}{1-R} \tag{3.14}$$

The transfer function between point 0 and point 3 can be expressed as:

$$H_{03} = \frac{p(3)}{p(0)} = \frac{p(3)p(2)}{p(2)p(0)} = \frac{p(2)}{p(0)} H_{23} = \frac{e^{jkL} + Re^{-jkL}}{1+R} H_{23} \tag{3.15}$$

The four-pole transfer matrix of the sample is given as:

$$\begin{Bmatrix} P_0 \\ u_0 \end{Bmatrix} = \begin{bmatrix} \cos(k_c d) & jZ_c \sin(k_c d) \\ j\sin(k_c d)/Z_c & \cos(k_c d) \end{bmatrix} \begin{Bmatrix} P_3 \\ u_3 \end{Bmatrix} \tag{3.16}$$

If we assume the termination is rigid, u_3 will be equal to zero and the surface impedance can be expressed as:

$$Z_s = \frac{P_0}{u_0} = \frac{\cos(k_c d)}{j\sin(k_c d)/Z_c} = -jZ_c \cot(k_c d) \tag{3.17}$$

The transfer function between points 0 and 3 is

$$\frac{P_3}{P_0} = \frac{1}{\cos(k_c d)} = H_{03} \tag{3.18}$$

Setting Equations 3.15 and 3.18 equal to each other, one obtains:

$$H_{03} = \frac{e^{jkL} + Re^{-jkL}}{1+R} H_{23} = \frac{1}{\cos(k_c d)} \tag{3.19}$$

Thus, the complex wave number can be calculated using

$$k_c = \frac{1}{d} cos^{-1}\left(\frac{1+R}{e^{jkL} + Re^{-jkL}}\right) H_{23} \tag{3.20}$$

Setting equations 3.14 and 3.17 equal to one another,

$$Z_s = Z_0 \frac{1+R}{1-R} == -jZ_c \cot(k_c d) \tag{3.21}$$

and the characteristic impedance is:

$$z_c = jz_0 \frac{1+R}{1-R} \tan(k_c d) \tag{3.22}$$

3.3. Measurement of Flow Resistivity

Over 40 years ago, Delaney and Bazley (1970) developed empirical formulas which related the bulk properties to the flow resistivity of a material. In similar work, they found that the sound absorption curves of different densities of rock wool collapsed on themselves when plotted versus the non-dimensional frequency parameter $f\rho/\sigma$. In the intervening years, additional models were developed for fibers (Mechel, 2002) and plastic foams (Wu, 1988).

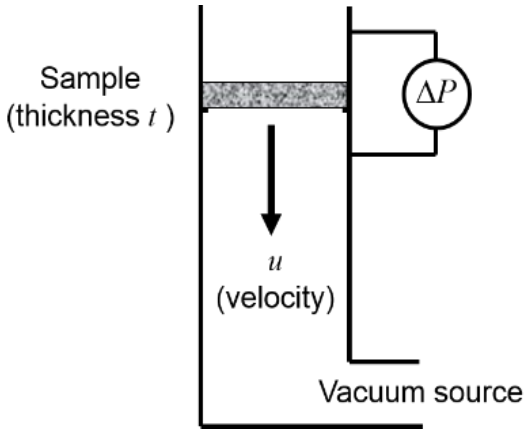

Figure 3.6 Schematic showing flow resistance measurement setup.

Determining the flow resistivity is comparatively less expensive than measurement using an impedance tube. Moreover, the measurement is comparatively easy. The measurement process has been standardized in ASTM C522. A schematic showing the testing apparatus is shown in Figure 3.6. And the testing apparatus at the University of Kentucky is shown in Figure 3.7. The static pressure drop ($\Delta \boldsymbol{p}$) across a sample is measured along with the flow velocity ($\boldsymbol{u}$). The flow resistivity can be expressed as

$$\sigma = \frac{\Delta p}{ut} \tag{3.23}$$

where t is the thickness of the sample.

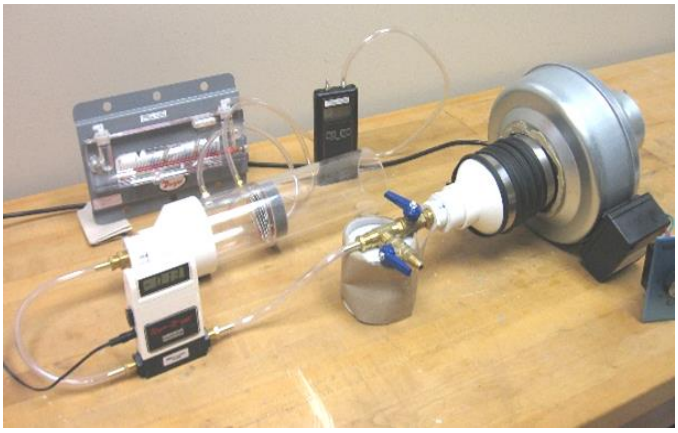

Figure 3.7 Flow resistance measurement apparatus.

Note that the quality of the estimated bulk properties depends on the measurement itself but also on the validity of the semi-empirical equation used. Many newer types of foam have flow resistivities in excess of 50,000 Rayls/m which are much higher than those used to develop the semi-empirical equations in the first place. Moreover, ASTM C522 indicates that the measurement procedure is intended for flow resistances below 10,000 Rayls. However, flow resistances beyond this limit are often measured. In spite of these limitations, the method is inexpensive and

simple, and provides sound absorption values that are acceptable to engineering accuracy for many industrial applications.

The semi-empirical equations are written in terms of the non-dimensional frequency parameter ($X = f\rho/\sigma$). Mechel (1988) improved the Delaney and Bazley (1970) model for fibers. The bulk properties are expressed as

For $X \leq 0.025$

$$k_c/k = (1 + 0.136X^{-0.641}) - j0.322X^{-0.502} \tag{3.24a}$$

$$z_c/z = (1 + 0.081X^{-0.699}) - j0.191X^{-0.556} \tag{3.24b}$$

For $X > 0.025$

$$k_c/k = (1 + 0.103X^{-0.716}) - j0.322X^{-0.663} \tag{3.24c}$$

$$z_c/z = (1 + 0.0563X^{-0.725}) - j0.127X^{-0.655} \tag{3.24d}$$

The limits for Mechel's model are $0.002 < X < 0.5$ though the model is sometimes used beyond this range in practice.

Wu (1988) developed the similar model for plastic foams that follows.

$$k_c/k = (1 + 0.188X^{-0.554}) - j0.163X^{-0.592} \tag{3.25a}$$

$$z_c/z = (1 + 0.209X^{-0.548}) - j0.105X^{-0.607} \tag{3.25b}$$

The limits for Wu's model are $0.01 < X < 0.83$ with $2{,}900 < \sigma < 24{,}300$.

3.4 Curve Fitting Methods

3.4.1 Curve Fitting to Determine Flow Resistivity

Simón et al. (2006) proposed using the measured absorption to determine the flow resistivity. The absorption is first measured using ASTM E-1050. Then, the flow resistivity is varied in the empirical equations (Equations 3.25a and 3.25b) until the least squares error is minimized. In so doing, a flow resistivity can be selected so that the sound absorption will best match the measurement. After that, the bulk properties can be determined using the empirical models of Mechel or Wu which were introduced previously. This method is attractive for a few reasons. First, there are several commercially available impedance tubes that are easy to use and sound absorption can be easily obtained. Moreover, this approach guarantees that the sound absorption will at least be correct at one thickness. On the other hand, the method again assumes that the empirical model is appropriate for the material measured.

3.4.2 Curve Fitting to Determine Biot Parameters

Similarly, the Johnson-Champoux-Allard (Allard, 2009) theoretical model can be used for the curve fit. The inputs to the model are the 5 Biot parameters (flow resistivity, porosity, tortuosity, thermal characteristic length, and viscous characteristic length). While flow resistivity is relatively easy to measure, the other 4 Biot parameters are difficult to measure and are only occasionally measured in industry. Pan and Jackson (Pan and Jackson, 2009) reviewed the methods for determining these parameters.

As an alternative, the Biot parameters can be estimated from the measured sound absorption coefficient. This procedure is used in the ESI Foam-X (ESI, 2007) software. The algorithm breaks the sound absorption into three frequency regimes (low, middle, and high) shown in Figure 3.8. The frequency regimes and the corresponding Biot parameters determined for each range are as follows.

Low Frequencies – Flow resistivity, porosity, and thermal characteristic length.

Middle Frequencies – Flow resistivity, viscous characteristic length, and tortuosity.

High Frequencies – Porosity, thermal characteristic length, and viscous characteristic length.

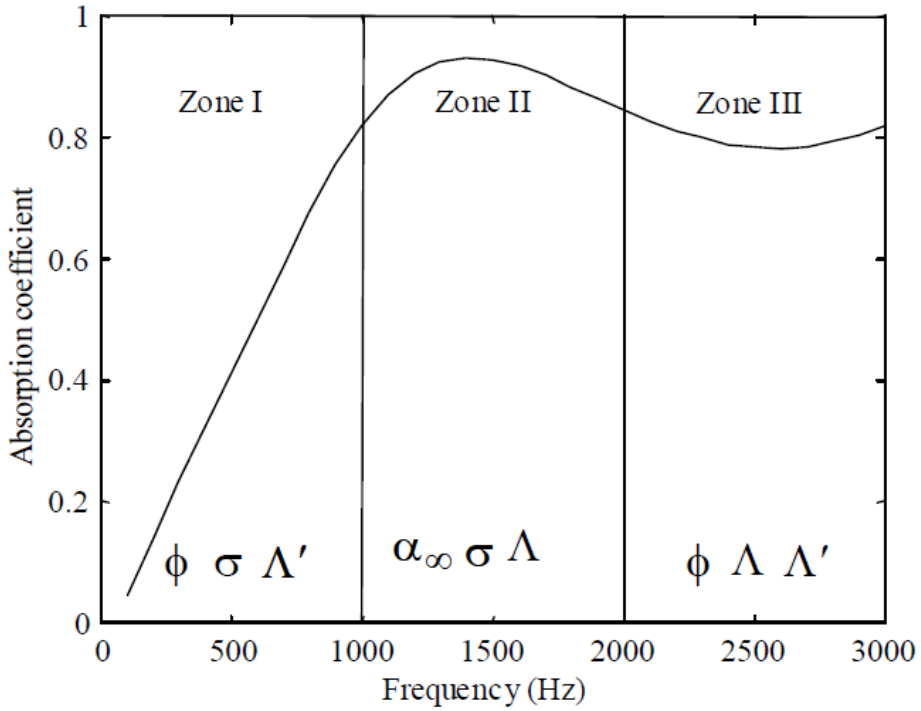

Figure 3.8 Frequency zones of a typical sound absorption coefficient.

3.5 Summary

This chapter surveys several approaches to determine the bulk properties (complex wavenumber and characteristic impedance) for sound absorbing materials. These approaches can be broken down into two classes; 1) direct and 2) indirect approaches. Details of each method were introduced.

CHAPTER 4 BULK PROPERTIES RESULTS AND COMPARISON

4.1 Direct Measurement Results

Three direct measurement approaches (two load, two cavity and three microphone method) to measure the bulk properties of porous materials were introduced in the previous chapter. In the following sections, results between the three approaches are compared for melamine foam and glass fiber.

4.1.1 Determination of Sound Absorption and Transmission Loss

Once the characteristic impedance and complex wave number have been determined, the transfer matrix can be expressed as

$$\begin{Bmatrix} P_1 \\ u_1 \end{Bmatrix} = \begin{bmatrix} A & B \\ C & D \end{bmatrix} = \begin{bmatrix} \cos(k_c d) & jZ_c \sin(k_c d) \\ j\sin(k_c d)/Z_c & \cos(k_c d) \end{bmatrix} \begin{Bmatrix} P_2 \\ u_2 \end{Bmatrix} \tag{4.1}$$

The sound absorption coefficient can be found in the following way. Assume a rigid termination so that u_2 = 0. In that case, the normal incidence impedance can be expressed as

$$Z = \frac{A}{C} = \frac{z_c \cos(k_c d)}{j sin(k_c d)} \tag{4.2}$$

The reflection coefficient and sound absorption coefficient can be wrote as

$$R = \frac{Z - 1}{Z + 1} \tag{4.3}$$

and

$$\alpha = 1 - |R|^2 \tag{4.4}$$

respectively. In addition, the transmission loss can be expressed directly in terms of the transfer matrix terms as

$$TL = 20log_{10}\left|A + \frac{B}{\rho c} + C\rho c + \frac{D}{2}\right| \quad (4.5)$$

4.1.2 Results for Foam

The characteristic impedance and complex wave number determined using the three direct measurement approaches is shown in Figures 4.1 and 4.2 for a 1 inch thick 0.6 lbs/ft^3 melamine foam. Figure 4.1 shows the real and imaginary characteristic impedance. Results between the three approaches agree above 800 Hz though there are some differences below 800 Hz. Figure 4.2 shows similar results for the complex wave number. Results agree over the entire frequency range.

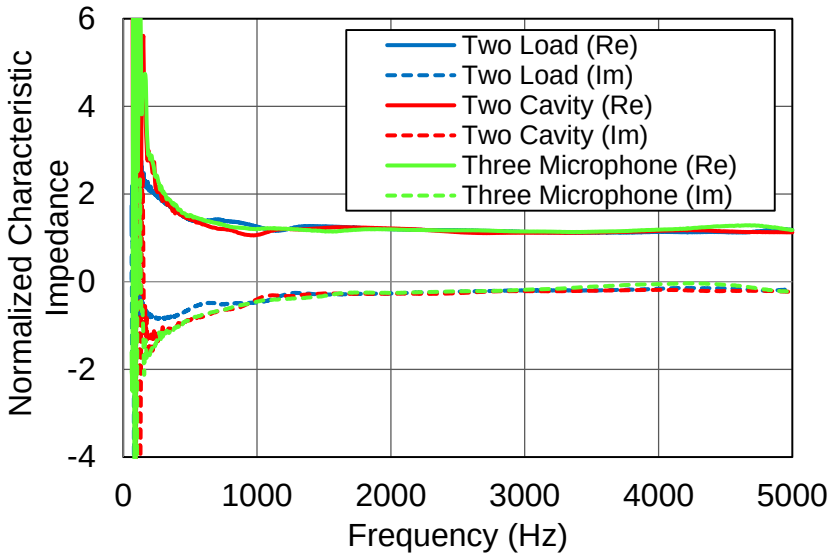

Figure 4.1 Direct measurement results of characteristic impedance for 1 inch 0.6 lbs/ft^3 melamine foam.

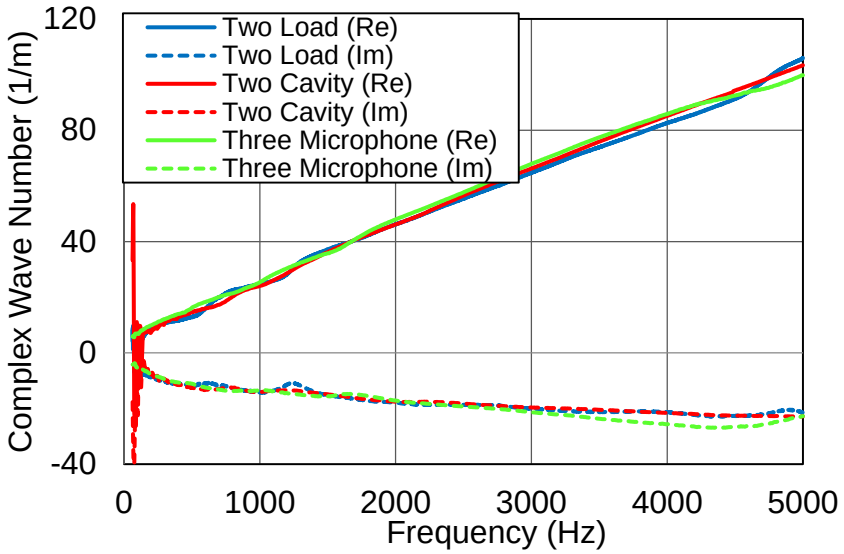

Figure 4.2 Direct measurement results of complex wave number for 1 inch 0.6 lbs/ft^3 melamine foam.

The characteristic impedance and complex wave number were then used to calculate the sound absorption coefficient using Equations 4.1 through 4.4. The transmission loss was calculated using Equations 4.1 and 4.5. Results are compared for sound absorption and transmission loss in Figures 4.3 and 4.4 respectively.

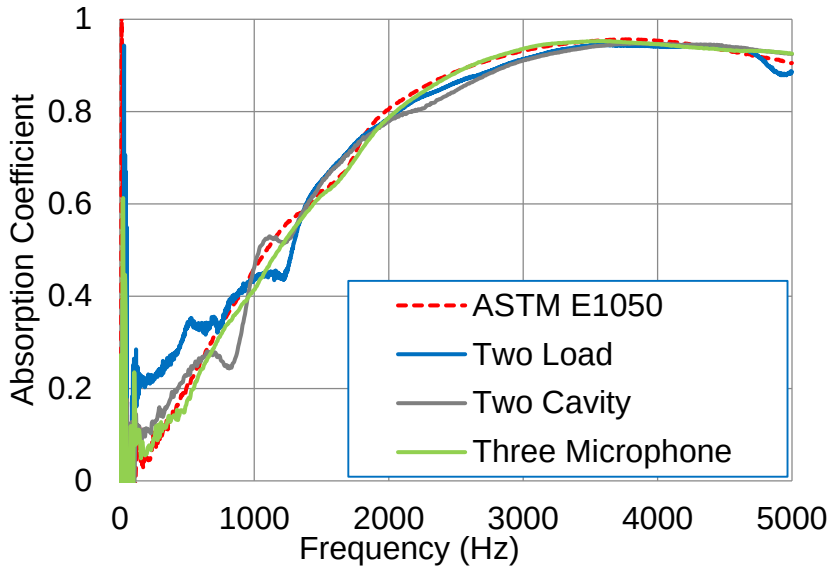

Figure 4.3 Direct measurement results of absorption coefficient for 1 inch 0.6 lbs/ft^3 melamine foam.

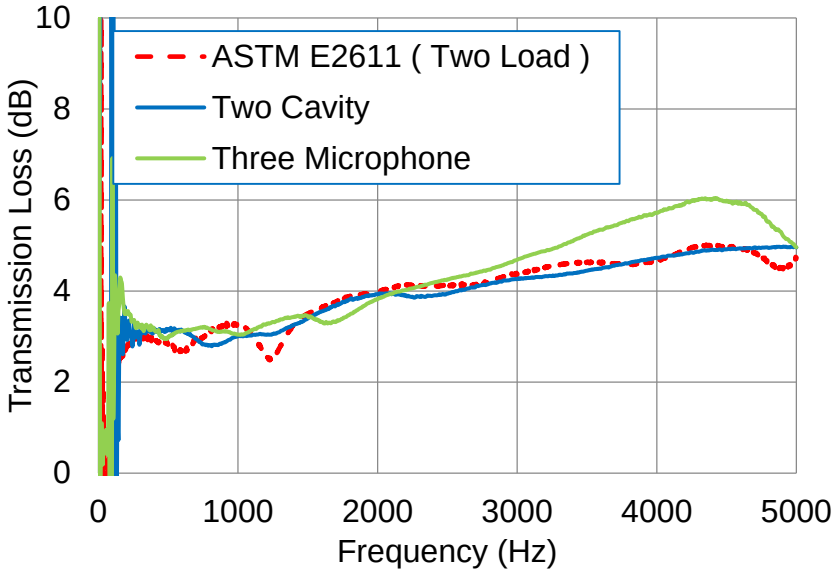

Figure 4.4 Direct measurement results of transmission loss for 1 inch 0.6 lbs/ft^3 melamine foam.

As shown in Figure 4.3, the sound absorption coefficient compares well above 1200 Hz and the three microphone method is smoother than the other two approaches. The three methods are also compared to the directly measured sound absorption coefficient for a 1 inch thick sample using ASTM E1050 with good agreement. The result shows that the three microphone method compares more closely with ASTM E1050 than the other methods. However, it is recognized that these are results for a single sample of a particular material so no general conclusions can be made.

Figure 4.4 shows similar comparisons for transmission loss. The two load method (ASTM E2611, 2009) is the approach that is commonly used to measure transmission loss directly. It can be seen that both the two cavity and three microphone results agree well though the three microphone results are a little smoother. However, the three microphone results are a little high above 2500 Hz which is due to differences in the imaginary part of the complex wave number.

4.1.3 Results for Fiber

A similar set of measurements was performed on a 1 inch thick 1 lbs/ft^3 glass fiber. Figures 4.5 and 4.6 show the characteristic impedance and complex wave number measured using the direct measurement approaches. The characteristic impedance compares well above 800 Hz though there are some differences at low frequencies. The complex wave number compares well over the entire frequency range.

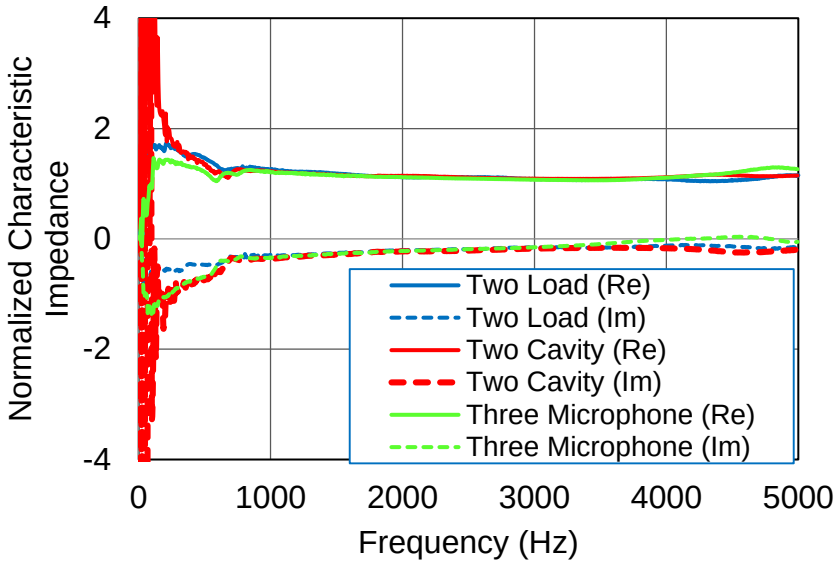

Figure 4.5 Direct measurement results of characteristic impedance for 1 inch 1.0 lbs/ft^3 glass fiber.

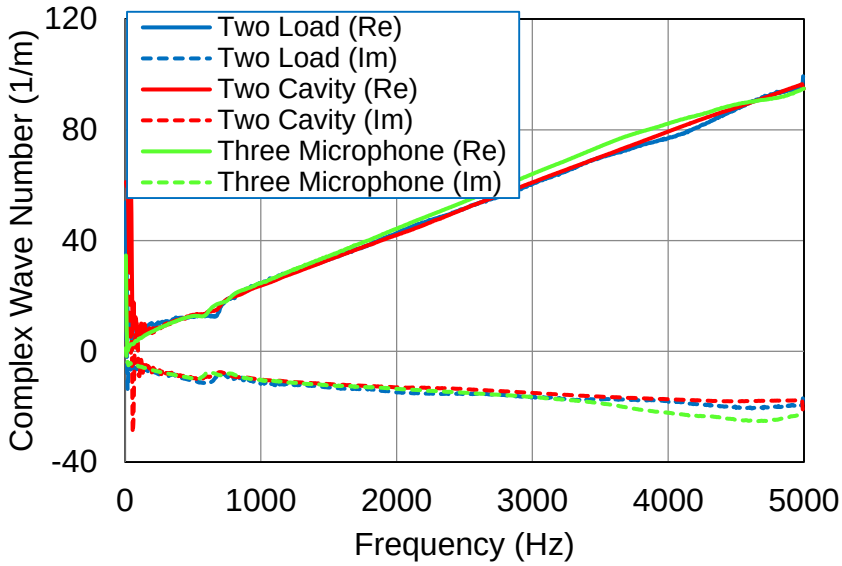

Figure 4.6 Direct measurement results of complex wave number for 1 inch 1.0 lbs/ft^3 glass fiber.

Figure 4.7 compares the sound absorption coefficient computed using each of the three direct methods to ASTM E1050. All three methods compare well over most of the frequency range. However, the sound absorption found using the two-load method determined properties is noisy and high at low frequencies. The three microphone method is the smoothest curve and compares best to the direct measurement (ASTM E1050).

Figure 4.8 compares the transmission loss computed using the two-cavity and three-microphone method to that measured directly by the two-load measurement. Once again, the curve obtained using the three microphone method is smoother. However, the two-cavity approach compares better with direct measurement (ASTM E2611) above 3000 Hz.

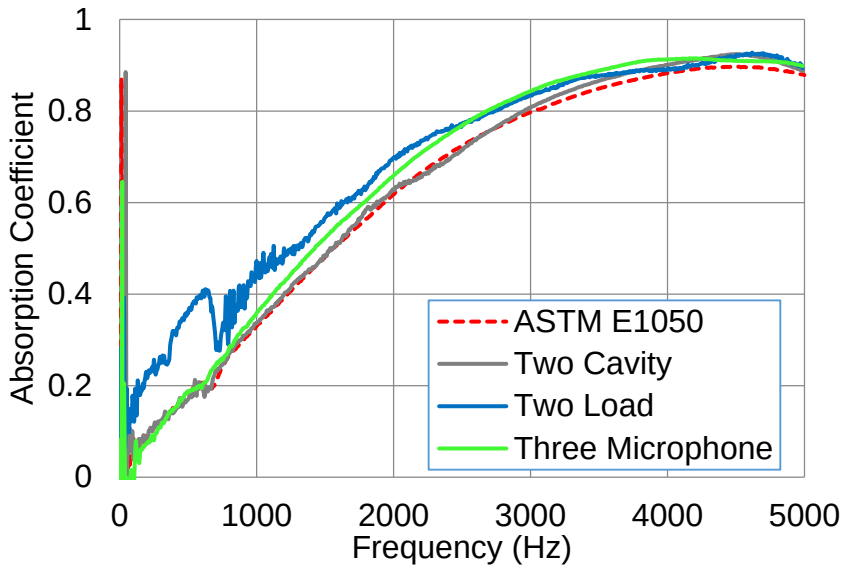

Figure 4.7 Measurement results of absorption coefficient for 1 inch 1.0 lbs/ft^3 glass fiber.

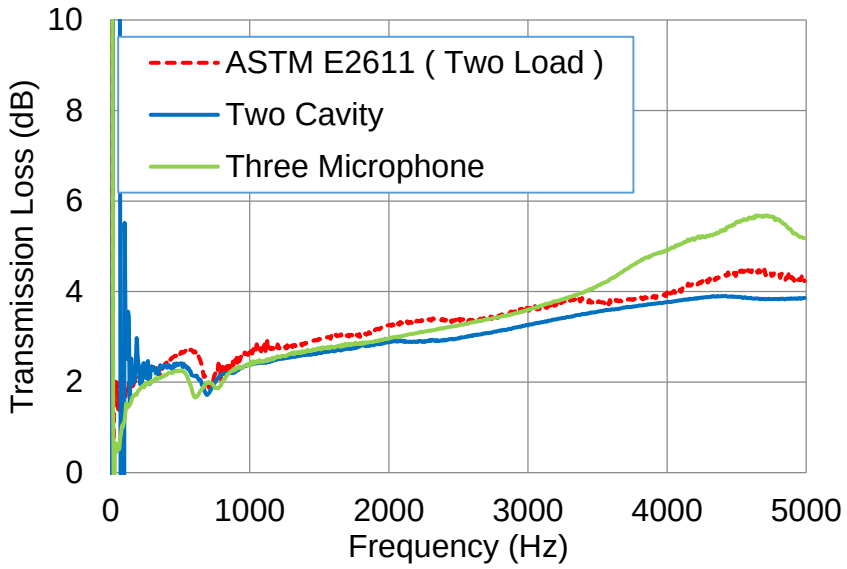

Figure 4.8 Measurement results of transmission loss for 1 inch 1.0 lbs/ft^3 glass fiber.

4.1.4 Direct Measurement Methods Comparison

The results suggest that the three microphone method should be recommended over the two cavity and two load approaches. There are a few reasons. First, the three microphone method is the simpler measurement approach. It requires only a single measurement. Secondly, results are smoother, especially at low frequencies, than the alternative methods.

4.2 Indirect Characterization Results

Three indirect characterization approaches to determine the bulk properties of porous materials were detailed in the prior chapter. These characterization approaches included a) direct measurement of the flow resistivity and use of empirical equations, b) measurement of the sound absorption and a curve fit to find the flow resistivity based on the empirical equation, and c) measurement of the sound absorption and curve fit to determine the Biot properties. These three methods were compared for melamine foam and glass fiber.

4.2.1 Results for Foam

Results are compared for the indirect measurement approaches in Figures 4.9 and 4.10 for 1 inch 0.6 lbs/ft^3 melamine foam. There is good agreement between each of the indirect approaches. It can be observed that these results generally compare well with the direct measurement as shown in Figures 4.11 and 4.12. However, note that the characteristic impedance determined using the curve fitted Biot parameters varies from the measured bulk properties at low frequencies.

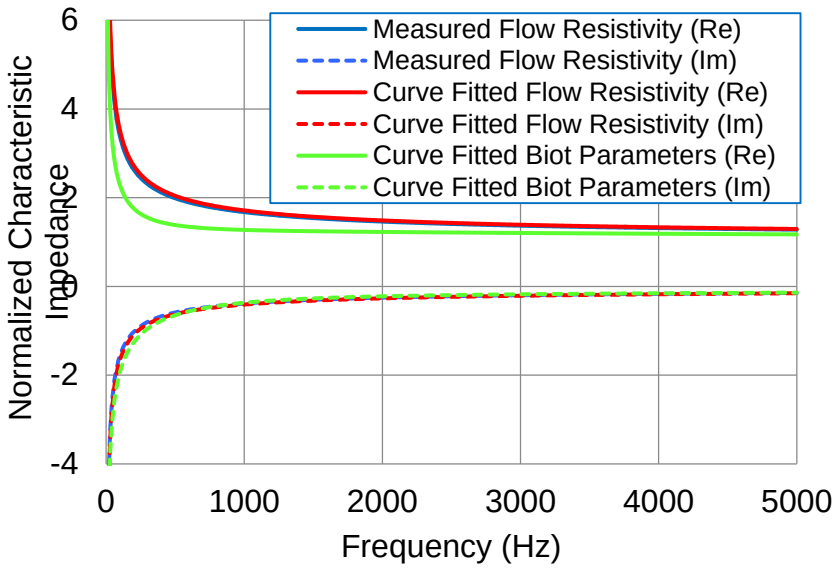

Figure 4.9 Indirect characterization results of characteristic impedance for 1 inch 0.6 lbs/ft^3 melamine foam.

The flow resistivities for melamine foam determined using direct measurement and determined by measuring the sound absorption coefficient and curve fitting to the empirical model of Wu (1988) are 12,100 Rayls/m and 11,400 Rayls/m respectively. When input into the empirical models, the difference between the bulk properties will be minimal as shown in Figures 4.9 and 4.10.

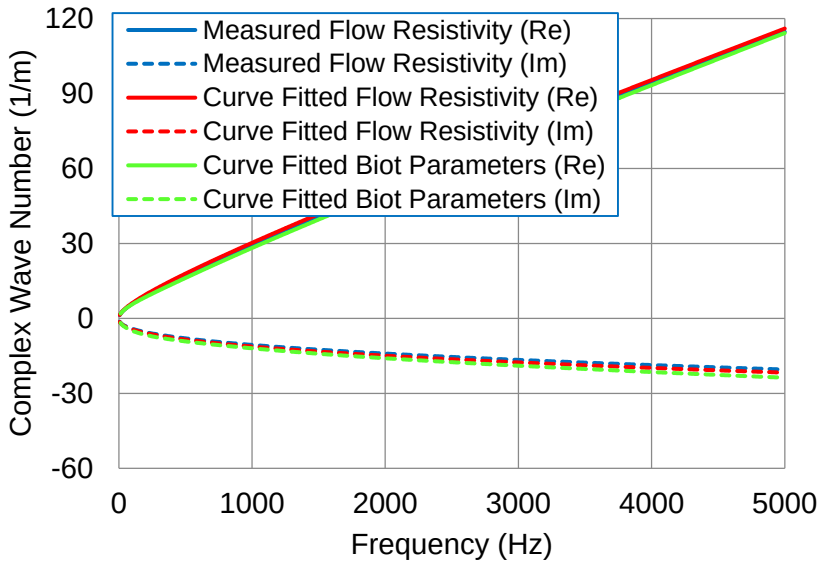

Figure 4.10 Indirect characterization results of complex wave number for 1 inch 0.6 lbs/ft^3 melamine foam.

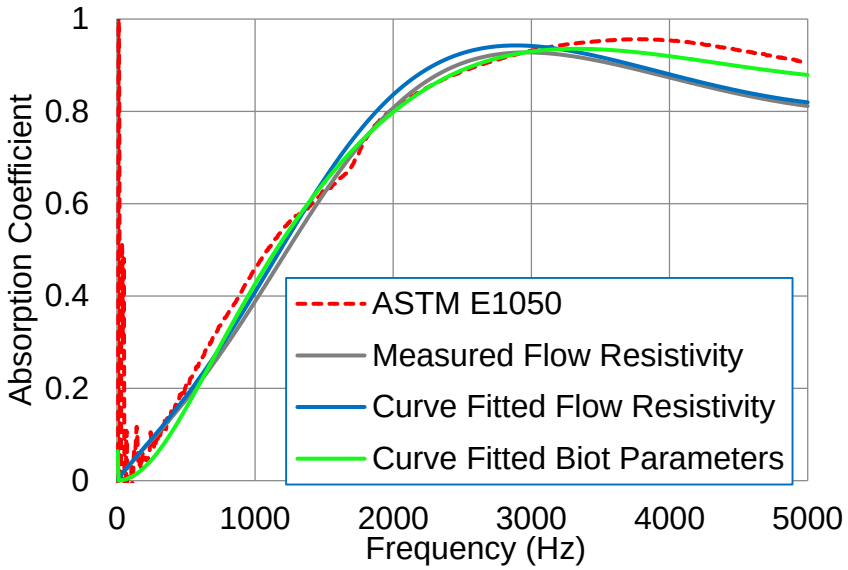

Figure 4.11 Indirect characterization results of absorption coefficient for 1 inch 0.6 lbs/ft^3 melamine foam.

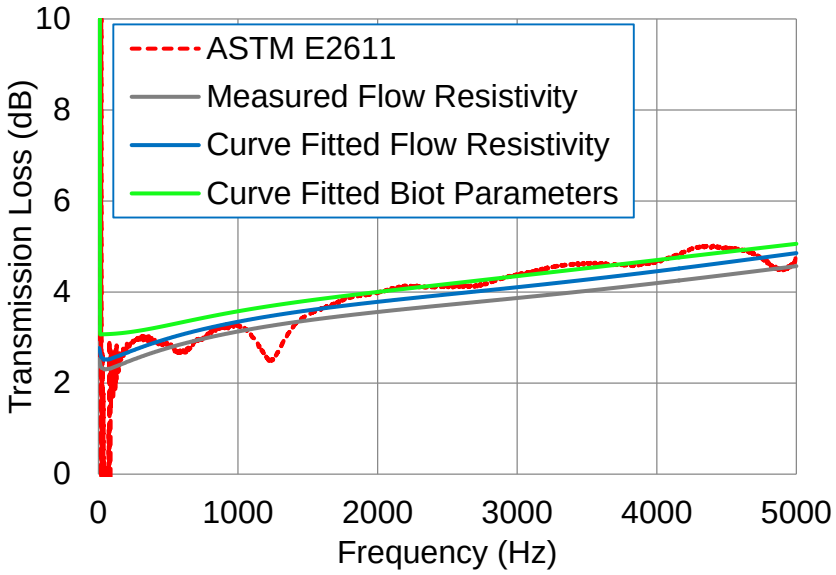

Figure 4.12 Indirect characterization results of transmission loss for 1 inch 0.6 lbs/ft^3 melamine foam.

The absorption coefficient and transmission loss for 1 inch 0.6 lbs/ft^3 melamine foam were determined using the bulk properties from the three indirect methods. Results are shown in Figures 4.11 and 4.12 respectively. The sound absorption coefficient and transmission loss agree well regardless of the indirect method used. This suggests that the differences in complex wave number and characteristic impedance are relatively unimportant. All indirect methods also compare well against direct measurement of both absorption coefficient (ASTM E1050) and transmission loss (ASTM E2611).

4.2.2 Results for Fiber

Figures 4.13 and 4.14 compare the characteristic impedance and complex wave number for a 1 inch thick 1 lbs/ft^3 glass fiber. There is good agreement between the three methods with only minor differences at low frequencies if the Biot parameters are curve fit. The flow resistivities determined using direct measurement and by measuring sound absorption and curve fitting to the empirical

model developed by Mechel (1988) are 7120 Rayls/m and 6700 Rayls/m respectively.

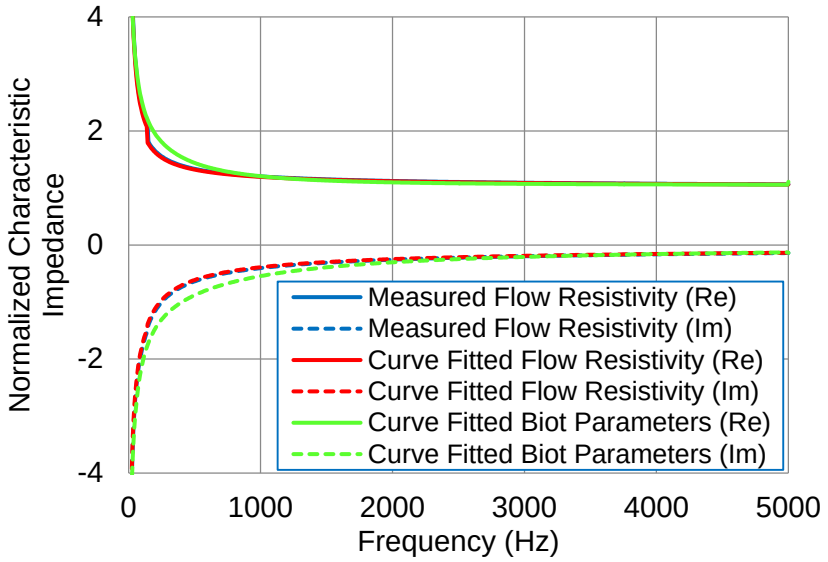

Figure 4.13 Indirect characterization results of characteristic impedance for 1 inch 1.0 lbs/ft^3 glass fiber.

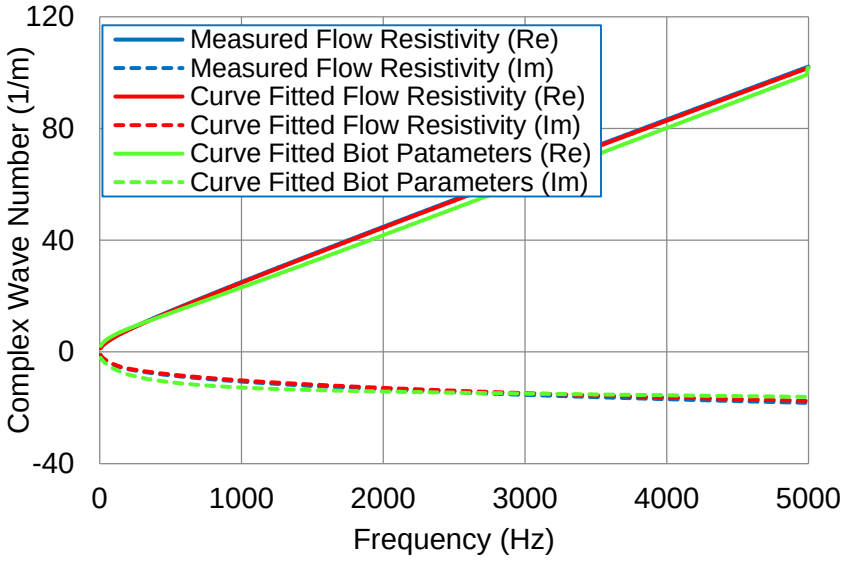

Figure 4.14 Indirect characterization results of complex wave number for 1 inch 1.0 lbs/ft^3 glass fiber.

Figures 4.15 and 4.16 compare the differences in predicted sound absorption and transmission loss. It is evident that there is little difference in the final result regardless of the approach used. The predicted sound absorption and transmission loss using the indirect approaches compare well with direct measurement using ASTM E1050 and ASTM E2611 respectively.

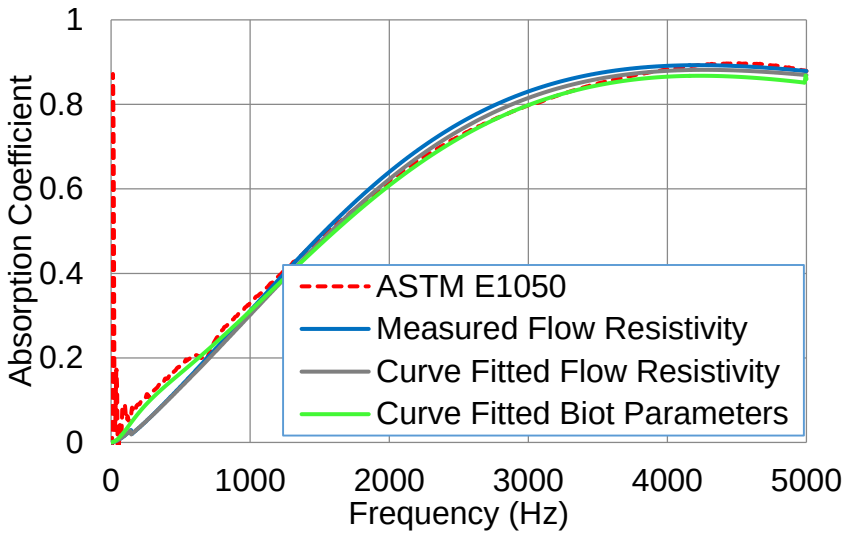

Figure 4.15 Indirect characterization results of absorption coefficient for 1 inch 1.0 lbs/ft^3 glass fiber.

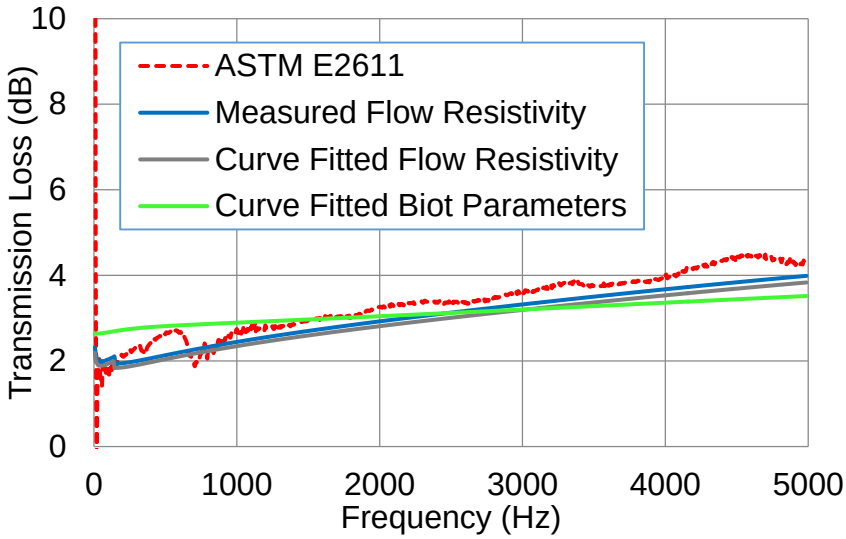

Figure 4.16 Indirect characterization results of transmission loss for 1 inch 1.0 lbs/ft^3 glass fiber.

4.2.3 Indirect Characterization Methods Comparison

Each of the three indirect characterization approaches compare well against each other for the melamine foam and glass fiber selected. However, it should be borne in mind that the flow resistivity approaches depend on the suitability of the empirical model for a given sound absorptive material. Though each of the three approaches are straightforward, direct measurement of the flow resistivity can be accomplished using a low cost system that is relatively easy to assemble. In addition, samples do not need to be as carefully prepared as those used in impedance tube tests.

4.3 Comparison

All six direct and indirect measurement methods can be categorized into three groups as shown in Figures 3.1 which are:

1. Direct measurement using an impedance tube.
2. Measuring the flow resistance and inputting the result into empirical equations.
3. Measurement of the sound absorption and curve fitting to determine the flow resistivity or the Biot parameters.

One approach from each group are selected and compared in Figures 4.17 and 4.18 for sound absorption coefficient and transmission loss respectively.

Figure 4.17 compares the sound absorption coefficient calculated by the bulk properties for 1 inch 1.0 lbs/ft^3 glass fiber. There is good agreement regardless of the method used.

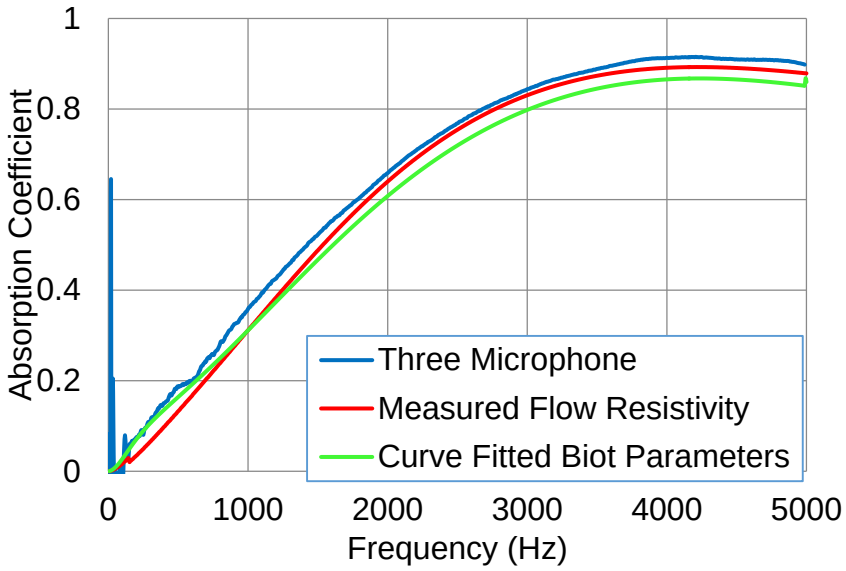

Figure 4.17 Absorption coefficient results comparison for 1 inch 1.0 lbs/ft^3 glass fiber.

Figure 4.18 compares the transmission loss for 1 inch 1.0 lbs/ft^3 glass fiber. The transmission loss compares well regardless of the approach used with some differences above 3000 Hz.

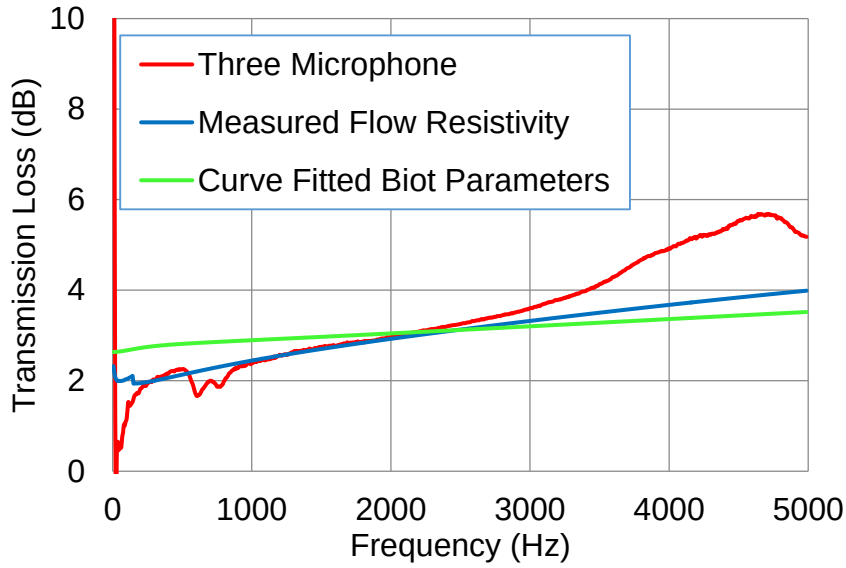

Figure 4.18 Transmission loss results comparison for 1 inch 1.0 lbs/ft^3 glass fiber.

4.4 Summary

The results indicate that each method is acceptable and the selection of the method will depend on the capabilities at hand. If an impedance tube is available, direct measurement using the three-microphone method is preferred though the two load and two cavity methods are certainly acceptable. If an impedance tube is not available, a flow resistivity measurement rig can be designed in accordance with ASTM C522 (ASTM, 2003) and the measured flow resistivity can be used in appropriate empirical equations. Alternatively, the sound absorption can be measured in accordance with ASTM E1050 (ASTM,1998) and the flow resistivity or Biot parameters that produce the best fit sound absorption using empirical or theoretical equations can be determined. Even though these approaches require an impedance tube, measurement of sound absorption is comparatively easier than direct measurement of the bulk properties.

CHAPTER 5 ACOUSTIC CHARACTERIZATION OF GLUES, COVERS AND DENSIFIED MATERIALS

5.1 Introduction

Allard and Atalla (2009) have detailed theoretical models for determining the sound absorption for layered materials, which include the response of both the frame and fluid. Similarly, Mechel (Mechel, 2008) has also developed both theoretical and empirical models describing porous absorbers. Though the models are implemented in different software packages, they have limited application to trim components for a number of reasons. Specifically, the models do not take into account:

1. Bonding agents such as glue and other adhesives.
2. Densified materials.
3. Compression of sound absorbing materials.

Though Allard and Atalla (2009) consider films, the properties of the film and the bonding of the film to the fiber are difficult to properly account for using the models. As a result, trim components are normally designed using a cut-and-try approach.

5.2 Effect of Glues, Covers and Compression

5.2.1 Effect of Glue

Glue is commonly used for bonding individual absorbing layers to one another or to a cover in sound absorbing materials. However, it is difficult to model or directly measure the acoustic properties of glue. Figures 5.1 and 5.2 show the effect of glue applied in between two glass fiber and foam layers respectively. Adding glue shifts the sound absorption peak to a lower frequency, but generally degrades the performance above 1000 Hz.

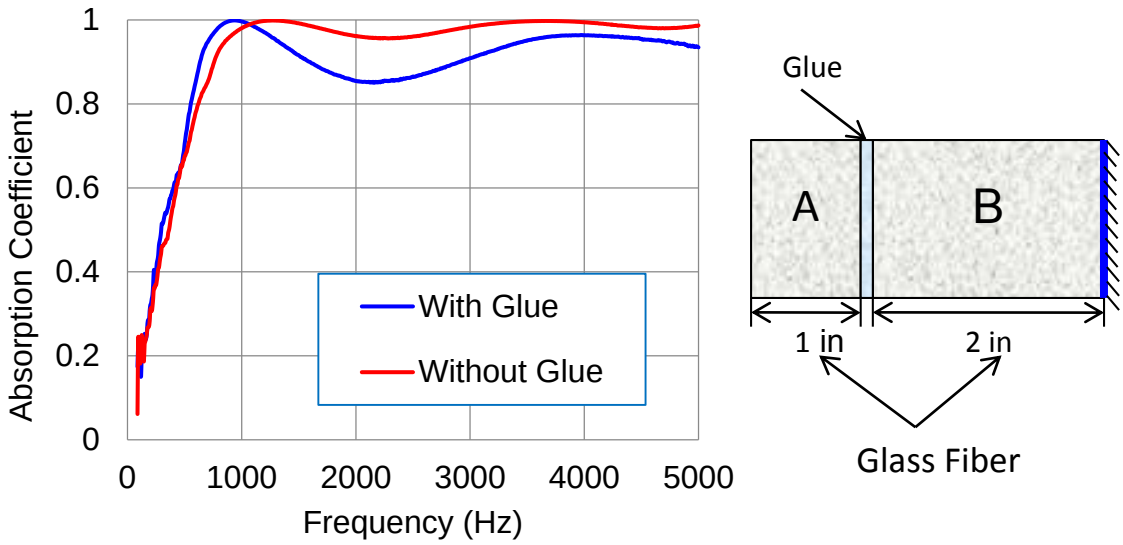

Figure 5.1 Effect of Glue between Two Glass Fiber Layers.

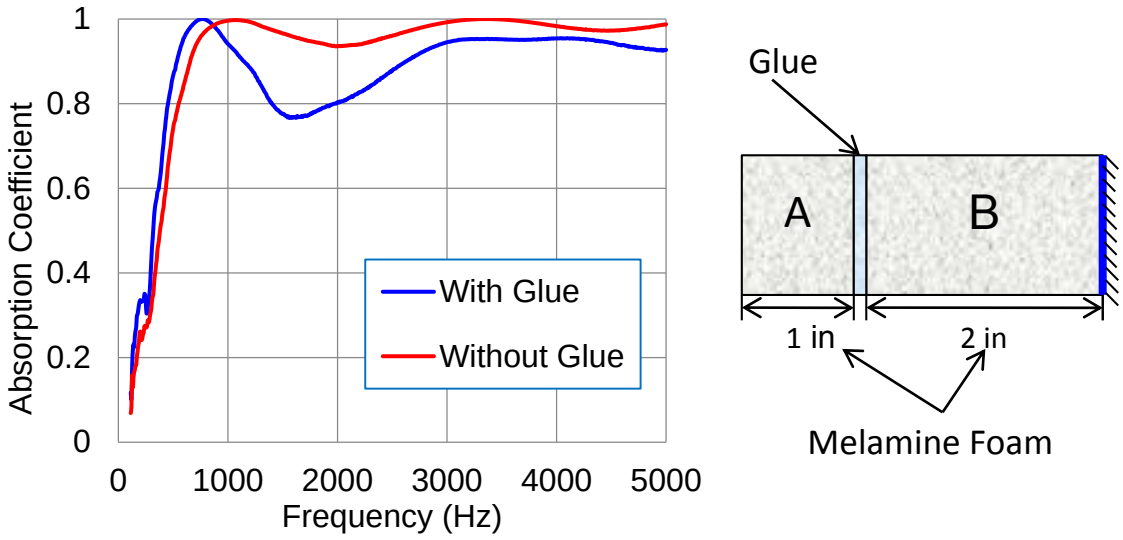

Figure 5.2 Effect of Glue between Two Foam Layers.

Figure 5.3 shows the effect of different coatings of glue. In this experiment, single, double and triple layers of glue were sprayed in between two foams and the sound absorption coefficient was measured using ASTM E1050 and compared. The results demonstrate that increasing the amount of glue further diminishes the performance above 1000 Hz.

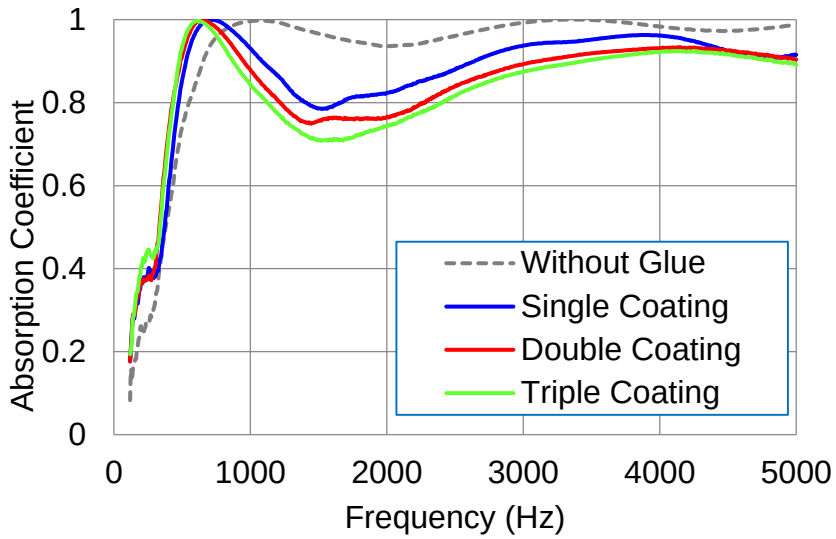

Figure 5.3 Effect of Coatings of Glue between Two Foam Layers.

5.2.2 Effect of Cover

Scrims or densified material layers are often used as covers. The acoustic properties of covers depend on their mounting. Sometimes the cover is bonded onto a porous material, and sometimes the cover is loosely attached and can be peeled away easily. Figure 5.4 shows the effect of a densified layer bonded to a glass fiber. The cover is a 1.5 mm 15.36 lbs/ft^3 high density glass fiber. Figure 5.5 shows the effect of a scrim placed in front of a glass fiber. In this case the scrim is not bonded to the material. Both figures indicate that covers improve the absorption coefficient at low frequencies but decrease the absorption at higher frequencies.

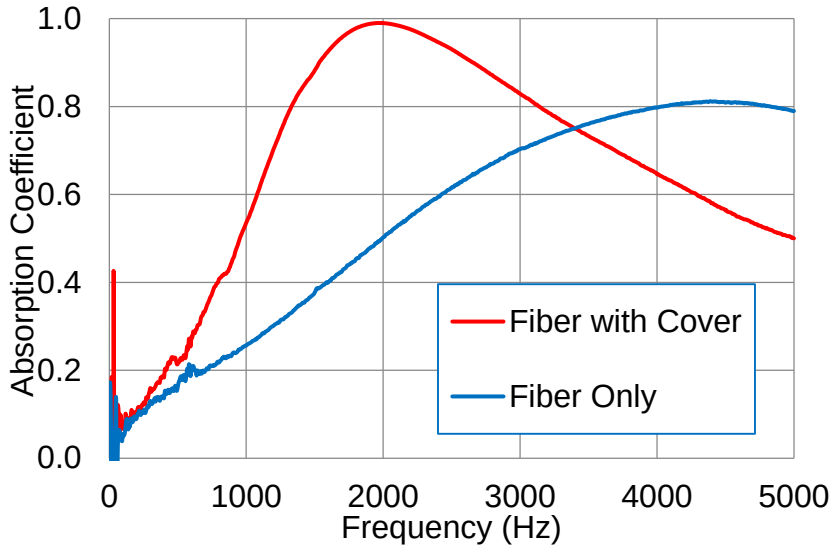

Figure 5.4 Effect of Densified Layer on Fiber.

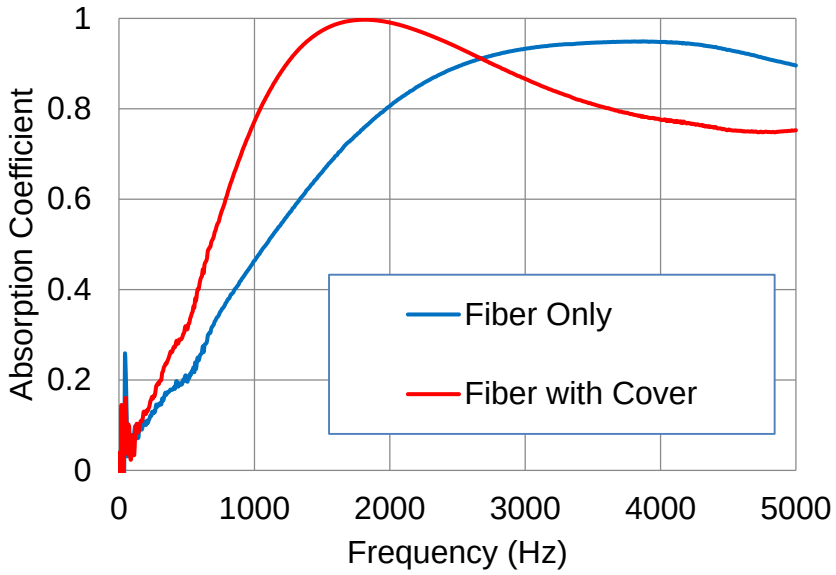

Figure 5.5 Effect of Scrim on Fiber.

5.2.3 Effect of Compression

The effect of compression was also investigated. A custom testing fixture was designed and used to measure compressed foam in the impedance tube using ASTM E1050.

As is shown in Figure 5.6, a mesh and a ring are used to compress foam evenly and hold it inside of the impedance tube. The total thickness of the mesh and ring is 0.1 inches. Figure 5.7 illustrates the procedure for compressing the sample in the holder. The procedure for mounting the sample is described as follows.

Step 1: Move the piston in the sample holder so that the depth in the holder is the intended thickness after the sample is compressed.

Step 2: Insert sample material in the sample holder.

Step 3: Compress the sample and then add mesh and ring in front of the sample to hold in place. Press the plastic ring so that it fits snugly in the impedance tube and holds the mesh in place.

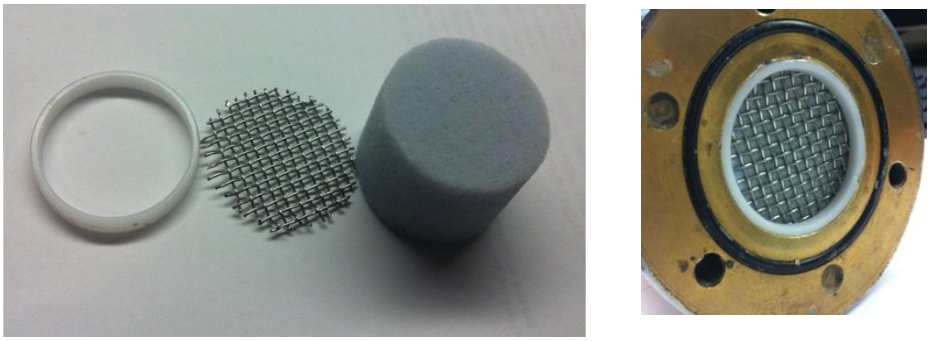

Figure 5.6 Schematic showing compression measurement procedure.

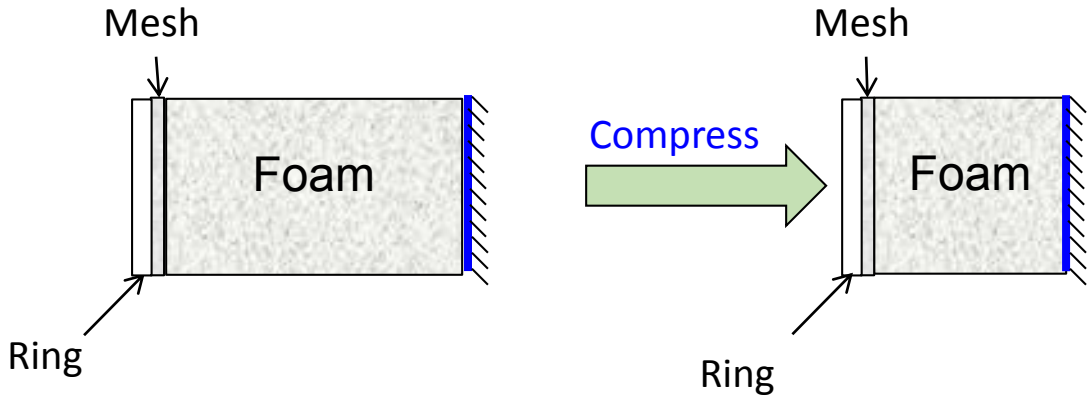

Figure 5.7 Schematic illustrating material compression procedure.

Before measuring compressed sound absorbing materials, the effect of the screen and ring were examined. A 1 inch foam was measured in the impedance tube using ASTM E1050. The measurement was then repeated with the screen and then with the ring and screen together. As we can see in Figure 5.8, adding a mesh in front of the foam has minimal impact on the sound absorption coefficient. Adding the ring has some effect above 3000 Hz but the impact is still minor.

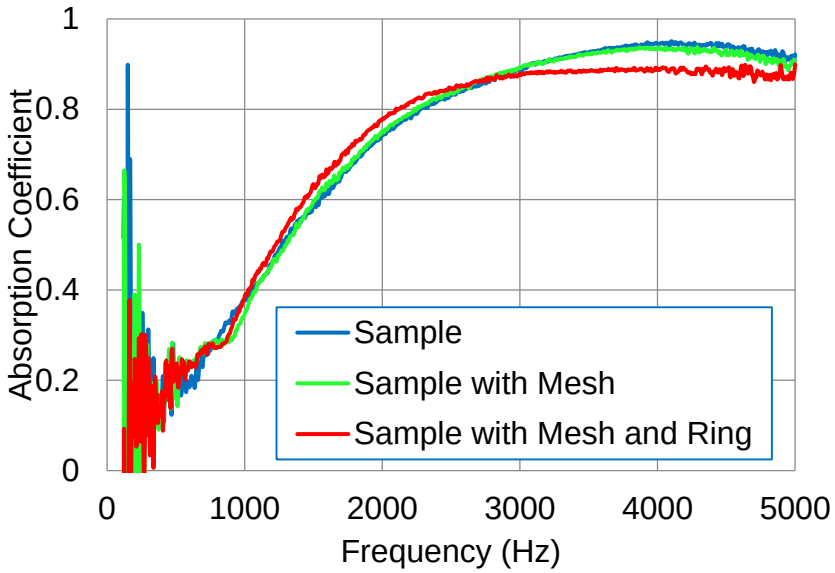

Figure 5.8 Effect of ring and screen on sound absorption.

A 1 inch foam was compressed to 0.75 inch, 0.5 inch, and 0.25 inch using the apparatus shown in Figure 5.6 and measured in the impedance tube using ASTM E1050. Results are shown in Figure 5.9. For this particular foam (1 inch thick and 0.6 lbs/ft^3), the absorption coefficient decreases over the entire frequency range. Also, additional shearing resonances in the solid matrix are evident due to the edge constraint (Song and Bolton, 2001).

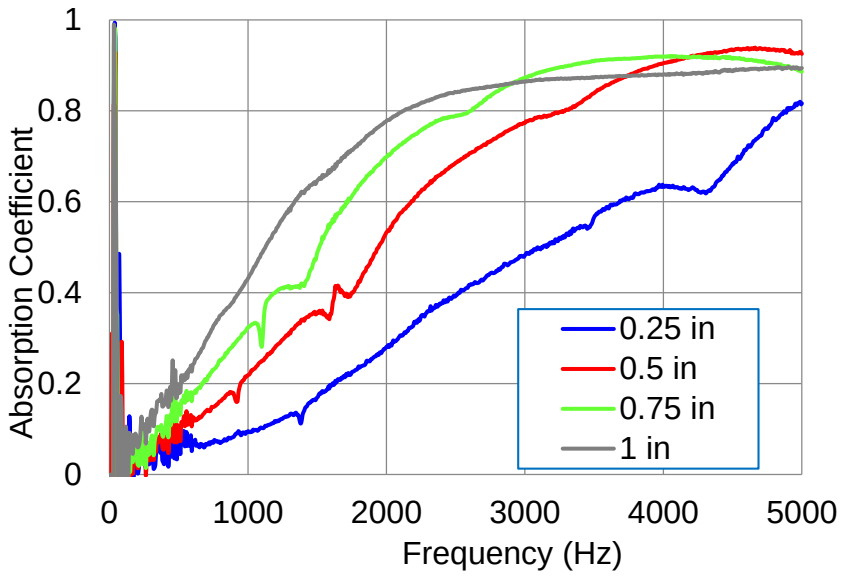

Figure 5.9 Effect of Compression of a 1 Inch 0.6 lbs/ft³ Foam.

Figure 5.10 compares the sound absorption coefficient of compressed and uncompressed 0.75 inch foam. The original blank for the compressed foam was 1 inch in thickness. For this particular foam, the sound absorption coefficient improves when it is compressed due to the increased density of the compressed foam. A similar comparison is shown in Figure 5.11 for a 1 inch foam that has been compressed to 0.25 inches. It is compared with 0.25 inch uncompressed foam. In both cases, an identical foam type and density was used for the compressed and uncompressed measurements. However, the foam samples were undoubtedly from different batches so there are likely some differences in the material.

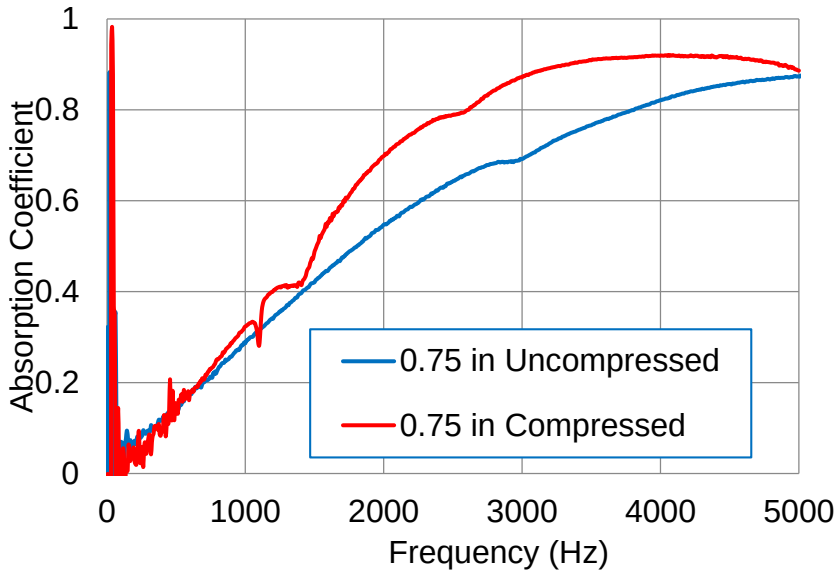

Figure 5.10 Effect of Compression of a 1 Inch 0.6 lbs/ft³ Foam.

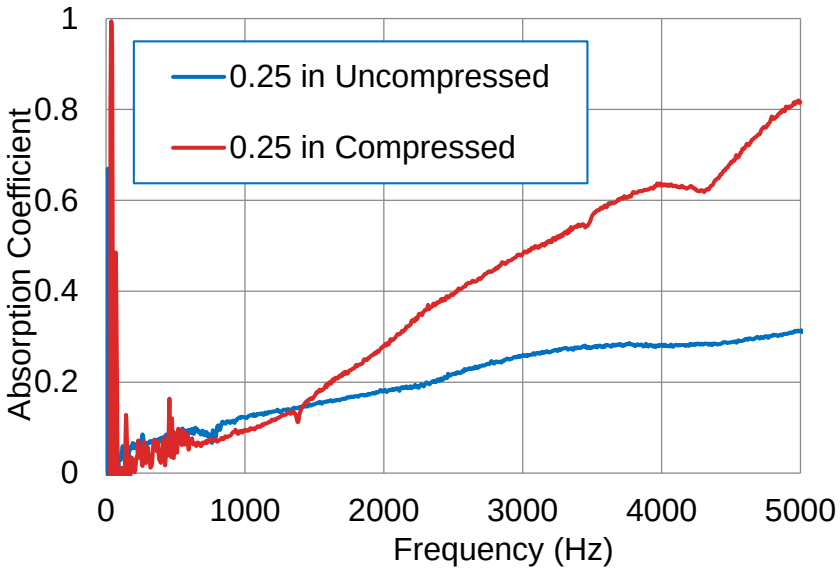

Figure 5.11 Effect of Compression of a 1 Inch 0.6 lbs/ft³ Foam.

5.3 Acoustic Characterization of Glues and Covers

5.3.1 Transfer Impedance Approach

A transfer impedance approach is commonly used to model perforates, covers and source impedance. A number of procedures have been used to measure the

transfer impedance of perforates. Ren and Jacobsen (1993) used an impedance tube with one microphone upstream and another downstream of the sample. Wu et al. suggested a simpler approach recognizing that the transfer impedance is simply a series impedance. The transfer impedance was determined by taking the difference between the impedances anterior and posterior to the perforate or cover. The impedance anterior to the perforate or cover is the combined impedance of the perforate or cover itself and the backing cavity. The impedance posterior to the cover is the impedance of the backing cavity alone. Both of these quantities can be measured using the two-microphone method and the transfer impedance is simply the difference between them.

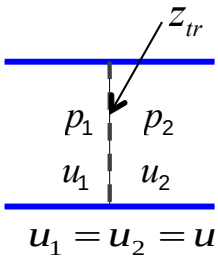

Figure 5.12 Schematic Illustrating Transfer Impedance.

The impedance difference method was used to measure the transfer impedance of covers and adhesive layers in the current work as shown in Figure 5.12. The sound pressure and particle velocity with and without the cover are p_1, u_1 and p_2, u_2, respectively.

Thus, the transfer impedance of a cover or perforate can be expressed as:

$$Z_{tr} = \frac{p_1 - p_2}{u} = Z_1 - Z_2 \tag{5.1}$$

Figures 5.13 through 5.15 shows how the transfer impedance can be measured in an impedance tube using the impedance difference approach. The impedance of the material was measured with (Z_2) and without (Z_1) the cover or bonding and the difference in impedances is the transfer impedance. The procedure shown in

Figures 5.13 has been used in the past for measuring panels or perforates. The setup shown in Figure 5.14 is suggested as an alternative for measuring adhesive layers, densified layers, and film covers. Figure 5.15 is an alternative way for measuring adhesive layers and covers where the sample is simply reversed. It is assumed in this particular case that the material is homogeneous. The material was measured with adhesive or cover first facing the source and then the sample is flipped. The advantage of using this method is that the same sample can be used for both tests without having to peel off the cover or densified layer.

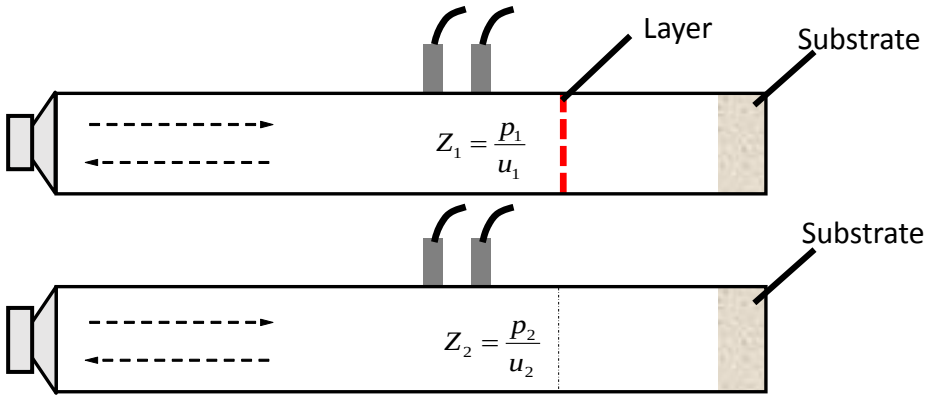

Figure 5.13 Transfer impedance measurement method 1 (a) Impedance with panel or perforate (b) Impedance without panel or perforate.

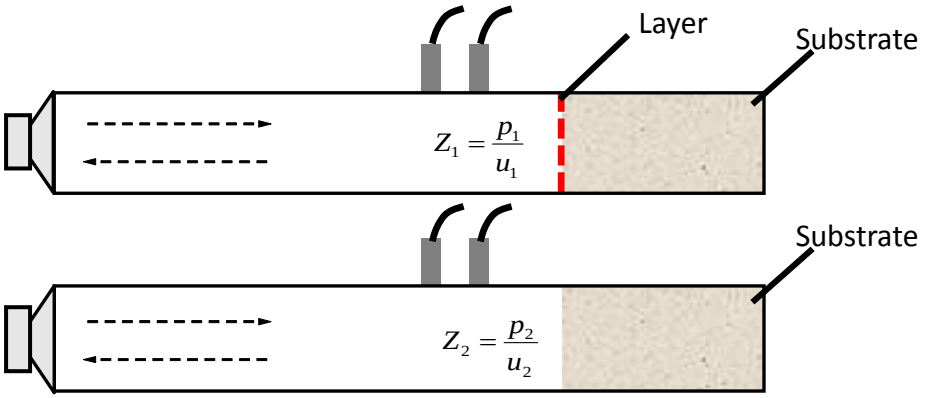

Figure 5.14 Transfer impedance measurement method 2 (a) Impedance with adhesive layer or bounded cover (b) Impedance without adhesive layer or bounded cover.

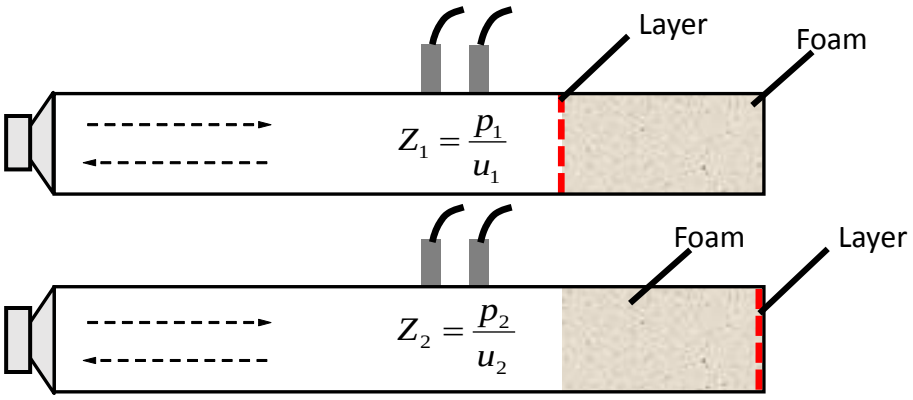

Figure 5.15 Transfer impedance measurement method 3 (a) Impedance with adhesive layer or bounded cover (b) Impedance without adhesive layer or bounded cover (sample flipped over to the other side).

Figure 5.16 show the transfer impedance results of a densified fiber layer measured using the three methods introduced above. The densified layer was bonded to a 1 inch homogeneous fiber. Method 2 and method 3 have good agreement with each other while method 1 is quite different from the other two methods. The results suggest that method 1 is not appropriate for measuring layers that are limp and bonded to the substrate material.

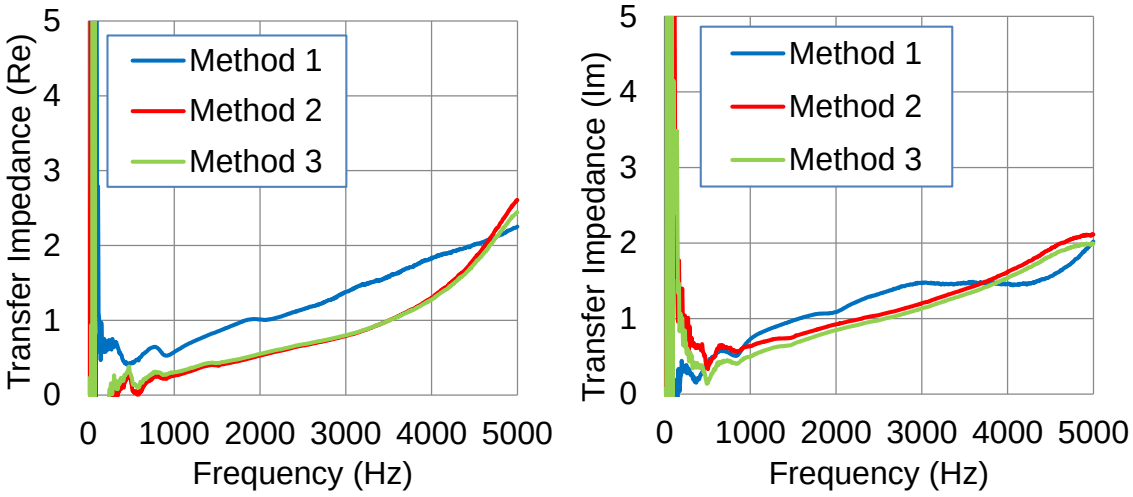

Figure 5.16 Transfer impedance result comparison using three measurement methods.

5.3.2 Transfer Matrix Approach

One of the most commonly used approaches for simulating the properties of a layered sound absorber is the transfer matrix approach (Munjal, 1987). The sound pressure and particle velocity on opposing sides of a sound-absorbing layer as shown in Figure 5.17 can be related to each other via

$$\begin{Bmatrix} p_1 \\ u_1 \end{Bmatrix} = \begin{bmatrix} \cos(k_c L) & jz_c \sin(k_c L) \\ j/_{z_c} \sin(k_c L) & \cos(k_c L) \end{bmatrix} \begin{Bmatrix} p_2 \\ u_2 \end{Bmatrix} \tag{5.2}$$

where k_c is the complex wavenumber, z_c is the characteristic impedance, and L is the length of the sample. The transfer matrix for a perforate or cover can be expressed in terms of the transfer impedance as

$$\begin{Bmatrix} p_1 \\ u_1 \end{Bmatrix} = \begin{bmatrix} 1 & z_{tr} \\ 0 & 1 \end{bmatrix} \begin{Bmatrix} p_2 \\ u_2 \end{Bmatrix} \tag{5.3}$$

where it is assumed that the particle velocity is equal on each side of the element and the transfer impedance is defined as

$$z_{tr} = \frac{p_1 - p_2}{u_1} \tag{5.4}$$

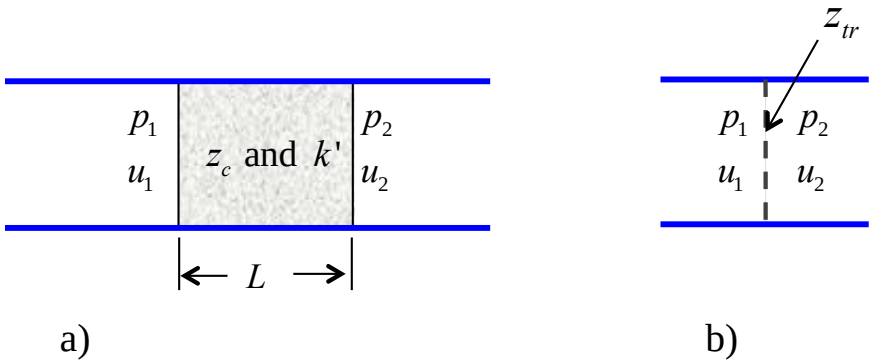

Figure 5.17 Schematic illustrating transfer matrix for a) a foam or fiber absorber or b) a transfer impedance.

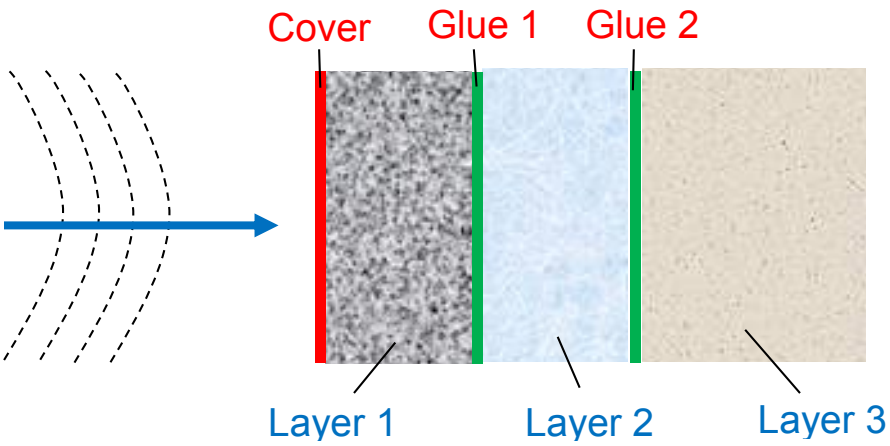

Figure 5.18 Schematic illustrating multi-layered materials.

Once transfer matrices are obtained for each element, the transfer matrix ($[T]$) for the complete absorber (Figure 5.18) can be combined by matrix multiplication. Accordingly,

$$[T] = \begin{bmatrix} T_{11} & T_{12} \\ T_{21} & T_{22} \end{bmatrix} = [T_1][T_2][T_3] \dots [T_n] \tag{5.5}$$

where $[T_i]$ is the transfer matrix for the i^{th} layer. The impedance of the sample can be expressed as

$$Z = r_n + x_n j = \frac{T_{11}}{T_{21}} \tag{5.6}$$

where r_n and x_n are the real and imaginary parts of the impedance. The reflection coefficient R can be expressed as

$$R = \frac{Z - 1}{Z + 1} \tag{5.7}$$

And the normal incident sound absorption coefficient can be expressed as

$$\alpha = 1 - |R|^2 \tag{5.8}$$

5.3.3 Validation of Transfer Impedance Approach

5.3.3.1 Validation Procedure for Glue

The suggested transfer impedance approach was tested for glue or adhesive. The transfer impedance of glue or adhesive layer was measured first using the impedance difference approach. Then the measured transfer impedance was used to predict the case where the layer was placed on a thicker sample or used to bond two samples. The predictions were compared to direct measurement using ASTM E1050.

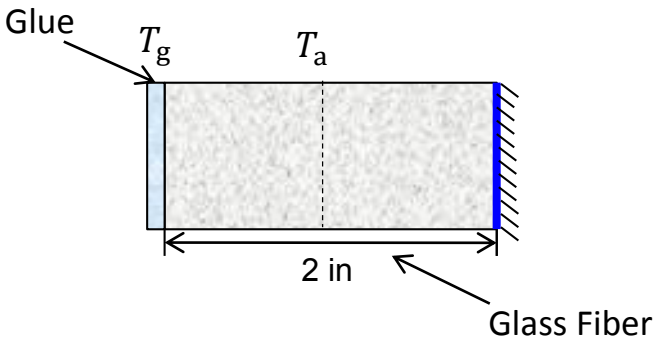

Figure 5.19 Schematic illustrating glue bonded to 2 inch glass fiber.

As shown in Figure 5.19, a layer of glue was initially applied on a 1 inch glass fiber, and the transfer impedance of glue (Z_{tr}) can be calculated using the impedance difference approach. The substrate material the glue was attached to was changed by adding another layer of 1 inch fiber posterior to the original sample. The bulk properties of the 2 inch glass fiber were measured using three microphone method prior to the glue application. The transfer matrix of glue (T_g) and fiber (T_a) can be calculated using Equations 5.2 and 5.3. And the absorption coefficient (α) of glue bonded to 2 inch glass fiber can be calculated then using Equations 5.5 to 5.8.

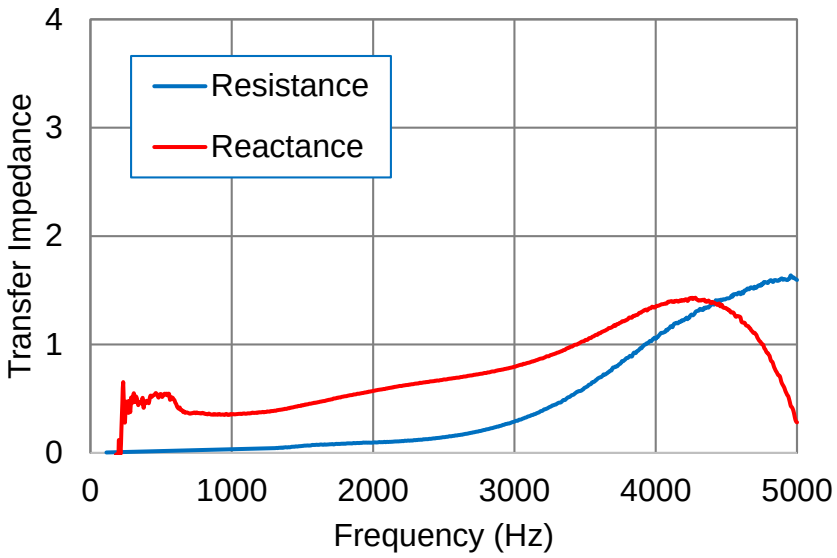

Figure 5.20 Transfer impedance of glue applied on glass fiber.

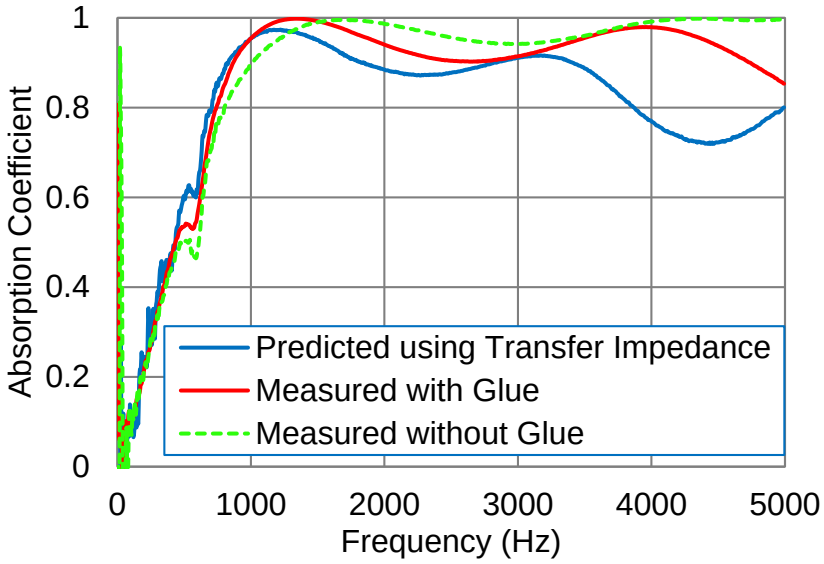

Figure 5.21 Comparison of sound absorption for glue bonded to 2 inch glass fiber.

Figure 5.20 shows the transfer impedance of glue measured using the impedance difference method. Figure 5.21 shows good agreement between the directly measured and predicted sound absorption for two 1 inch thick fibers with glue on the side facing the source below 3500 Hz. For comparison, the sound absorption without adhesive is also shown. Notice the good agreement between the predicted

and directly measured results which demonstrates that the transfer impedance approach can be used to determine the acoustic properties of glue applied to a porous material.

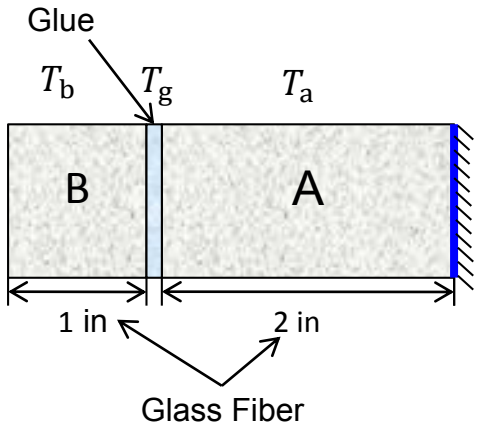

Figure 5.22 Schematic illustrating glue bonded between two glass fiber layers.

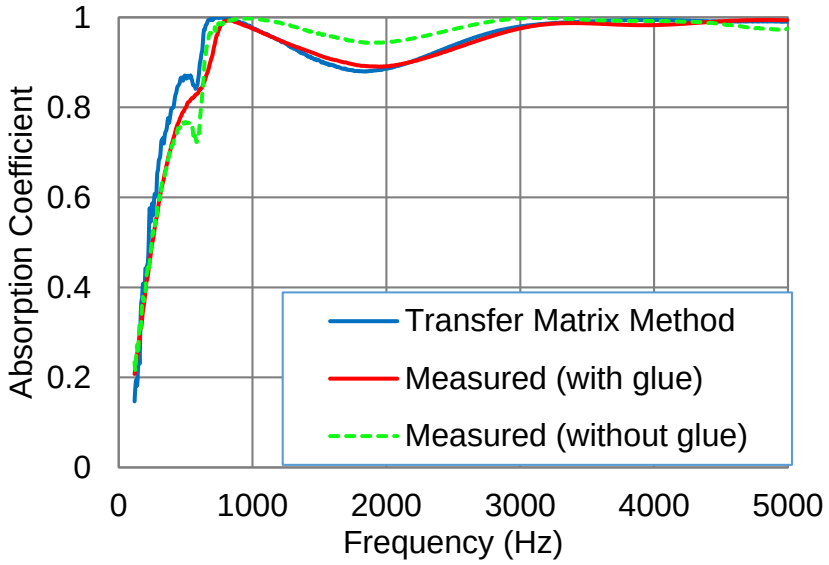

Figure 5.23 Comparison of sound absorption for glue bonded between two glass fiber layers.

Since glue is commonly used to bond two layers together, two layers of sound absorption with an adhesive between them was considered next and is illustrated in Figure 5.22. Glue is applied in between two layers A and B and the transfer

matrix T_g can be expressed using Equation 5.3. The transfer matrices (T_a and T_b) of layers A and B were measured using the three microphone method. Then, the sound absorption of the composite can be calculated using Equations 5.5 through 5.8 and compared with the result measured using ASTM E1050. Figure 5.23 compares the measured and transfer matrix predicted results with good agreement.

5.3.3.2 Validation Procedure for Cover

A validation example was considered where fiber was densified on one side to act as a facing. As shown in Figure 5.24, a densified layer was originally bonded to a 0.8 inch glass fiber. The transfer impedance of this densified cover was measured using the impedance difference method and the result is shown in Figure 5.25. The thickness of the glass fiber backing was then increased to 1.6 inches. The bulk properties for the 1.6 inch glass fiber were then measured using the three microphone method. The transfer matrix for the densified layer (T_g) and 1.6 inch glass fiber (T_a) was then calculated using Equations 5.2 and 5.3 and the sound absorption coefficient predicted using transfer matrix method.

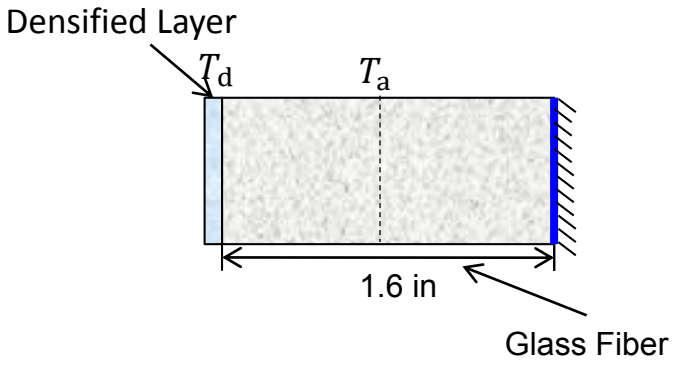

Figure 5.24 Schematic illustrating fiber with densified layer.

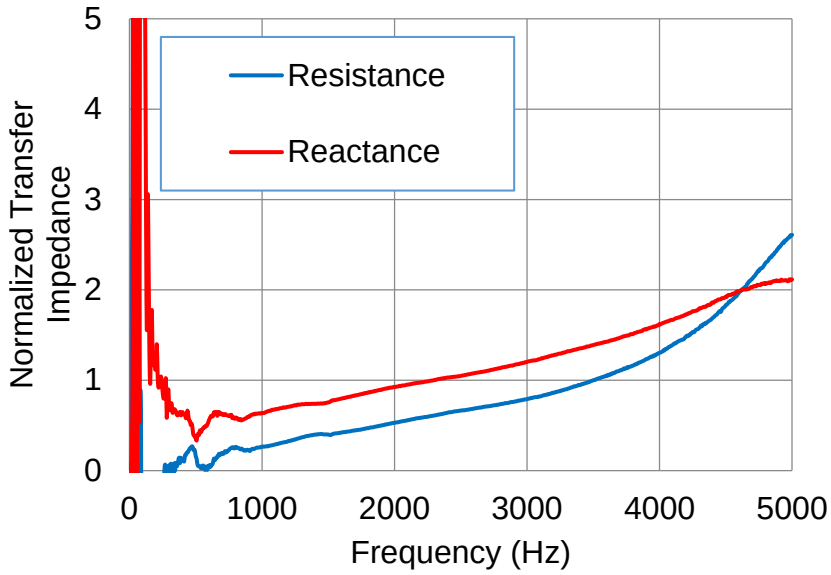

Figure 5.25 Transfer Impedance of Densified Layer.

Figure 5.26 shows good agreement between the directly measured and transfer matrix theory sound absorption. For comparison, the sound absorption without the densified layer is also shown. The results confirm that the transfer impedance approach can be used to model the acoustic properties of densified layer.

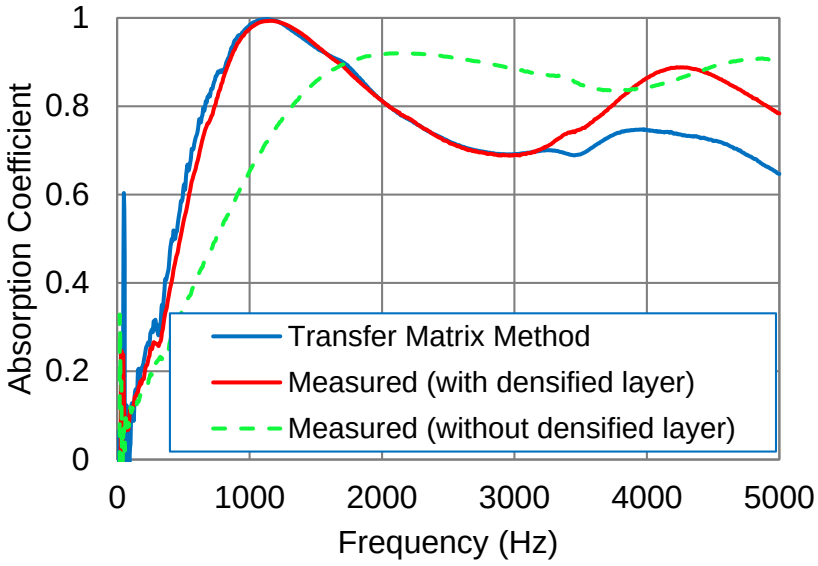

Figure 5.26 Comparison of sound absorption for fiber with densified layer.

5.4 Summary

The effect of covers, adhesives and compression of foams was investigated in this chapter. The transfer impedance of covers and adhesives was determined using an impedance difference approach. One way to validate the approach is to use the transfer matrix method to predict the absorption coefficient of a built-up sound absorber and compare with ASTM E1050. The good agreement between predicted and measured results suggest that the acoustic properties of the cover and adhesive can be measured using the suggested approach.

CHAPTER 6 TRANSFER IMPEDANCE RESULTS AND COMPARISON

6.1 Glue Transfer Impedance

6.1.1 Transfer Impedance of Increasing Levels of Glue

The transfer impedance for an adhesive (bonded to melamine foam) was measured using the procedure outlined in Chapter 5.3.1. Adhesive was weighed in 0.1-gram increments and then brushed onto the surface of the sample. Figure 6.1 shows the absorption coefficient of increasing levels of glue brushed on to the 0.5 inch 0.6 lbs/ft^3 melamine foam. The effect is similar to adding a film cover to a fiber or foam.

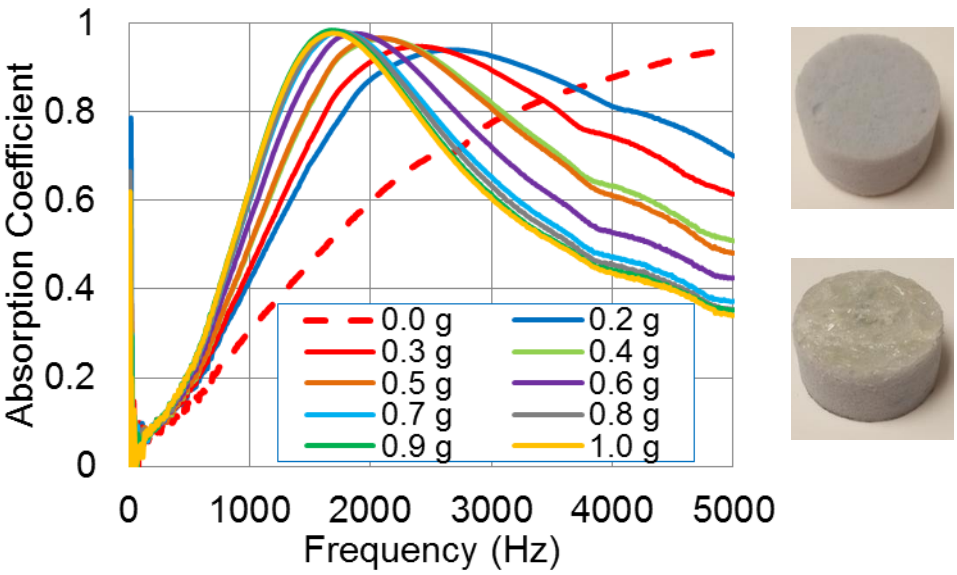

Figure 6.1 Sound absorption of increasing levels of glue brushed on to 0.6 lbs/ft^3 melamine foam.

The transfer impedance was measured after each brushing. The real and imaginary parts of the transfer impedance for different levels of glue are shown in Figures 6.2 and 6.3 respectively. Notice that the real part of the transfer impedance is roughly constant with frequency while the imaginary part increases linearly with

frequency. Brushing on additional layers of glue primarily increases the imaginary part of the transfer impedance (i.e., a mass effect). There is also some increase in the real part of the transfer impedance but the effect is less pronounced.

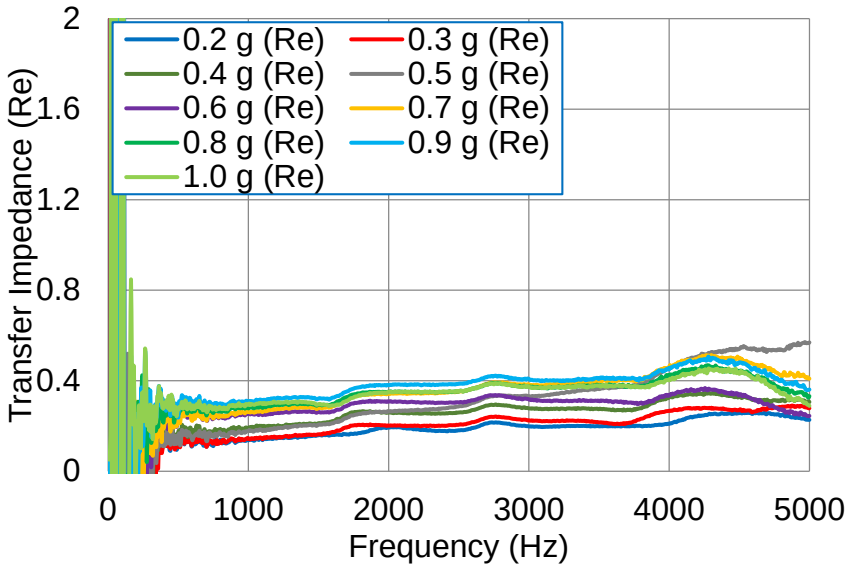

Figure 6.2 Transfer impedance (real part) of increasing levels of glue brushed on to 0.6 lbs/ft^3 melamine foam.

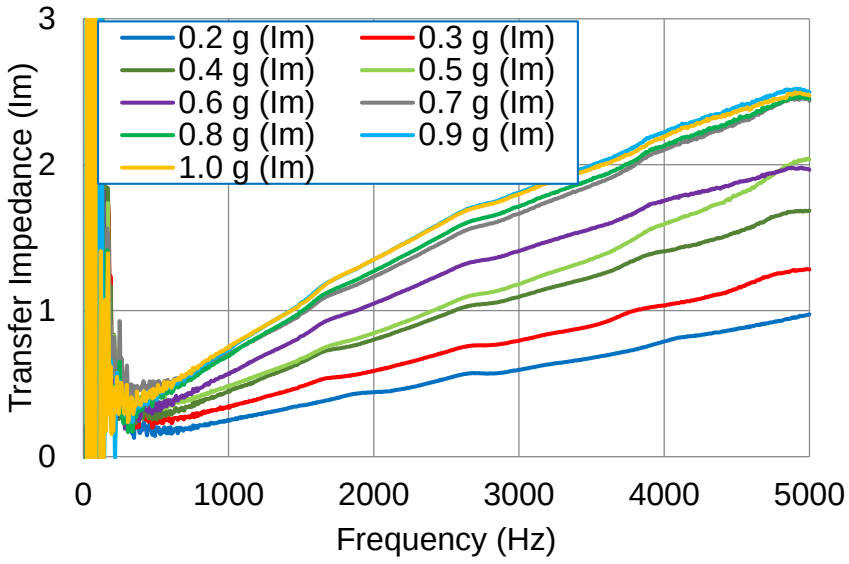

Figure 6.3 Transfer impedance (imaginary part) of increasing levels of glue brushed on to 0.6 lbs/ft^3 melamine foam.

6.1.2 Transfer Impedance of Glue Applied on Different Substrates

An equivalent mass of glue was applied to different substrates and the transfer impedance was measured. Substrates considered included melamine foam, polyester foam, and glass fiber.

Figure 6.4 and 6.5 show the real and imaginary parts respectively of transfer impedance for 0.6g of glue applied. Results show that the transfer impedance of the same amount of glue applied on different substrates are quite different. The main reason is due to glue application. The glue used in this test is a hot melted glue, and the glue was placed on a hot plate until it was melted and was carefully brushed on to the substrates. Glue can be easily and evenly applied to the surface of a melamine foam. However, it is difficult to brush the glue on to polyester and glass fiber. While glue completely covered the melamine, there were gaps in the coverage for the polyester and glass fiber. Note that the transfer impedance is highest for the melamine and lowest for the glass fiber.

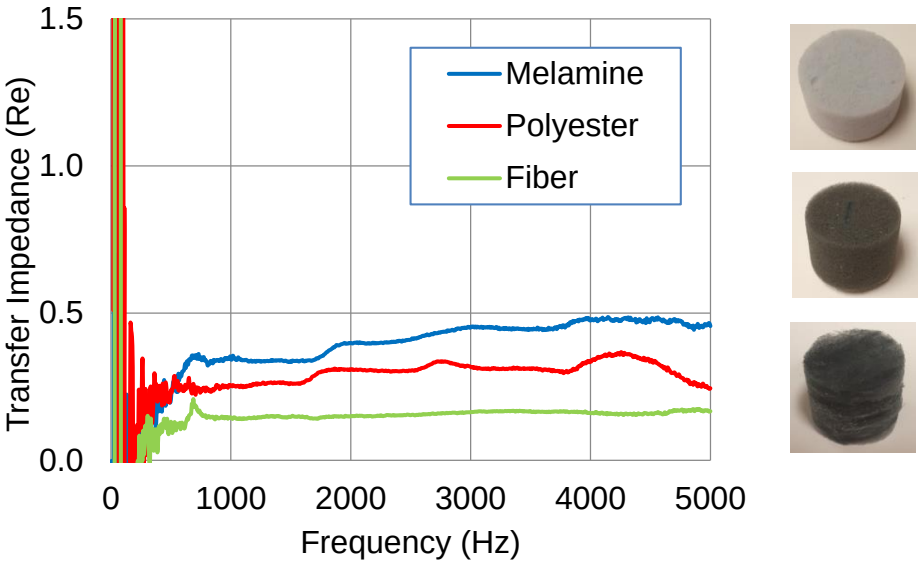

Figure 6.4 Transfer impedance (real part) of 0.6g glue applied different substrates.

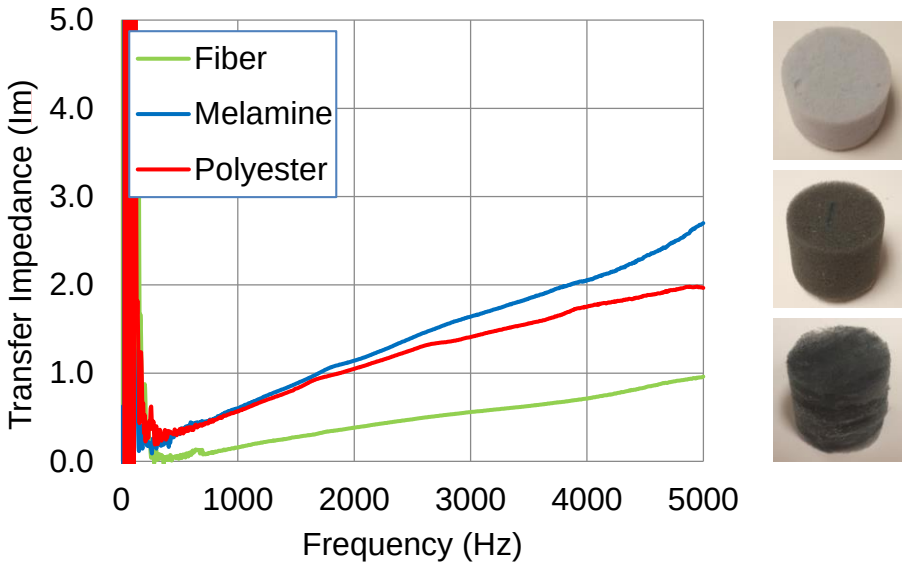

Figure 6.5 Transfer impedance (imaginary part) of 0.6g glue applied on different substrates.

6.2 Cover Transfer Impedance

6.2.1 Transfer Impedance of Cover and Perforated Panel

The transfer impedance for a cover and a perforated panel were measured using the procedure outlined in Section 5.3.1. The cover is made of armaglas fabrics which provides added heat protection and the perforated panel is made of steel with 0.35 porosity and a hole diameter of 0.1875 inch. Figure 6.6 shows a photograph of the cover and perforated panel.

Figure 6.6 Photograph of a) Cover (armaglas fabrics) b) Perforated panel (steel)

Figure 6.7 shows the effect in absorption coefficient of adding a cover and perforated panel to 1.2 inch glass fiber. The sound absorption coefficient was measured and averaged for 5 samples in each case.

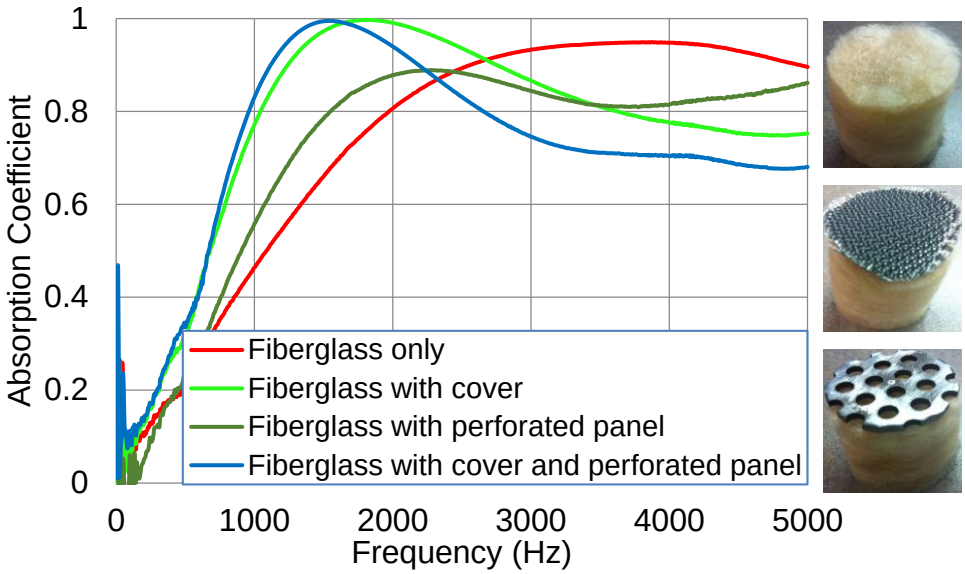

Figure 6.6 Sound absorption of 1.2 inch glass fiber with cover and perforated panel.

Figures 6.8 and 6.9 show the transfer impedance of a cover and a perforated panel respectively. Results were averaged for 5 samples.

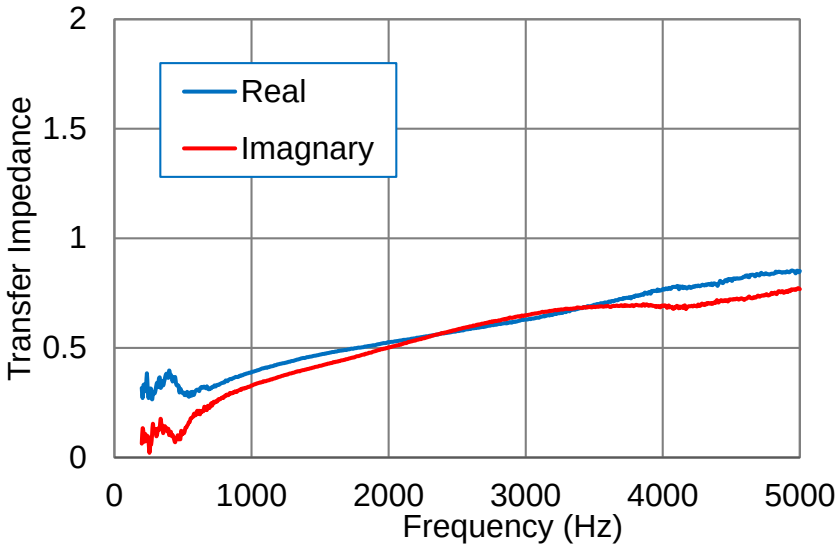

Figure 6.7 Transfer impedance of a cover.

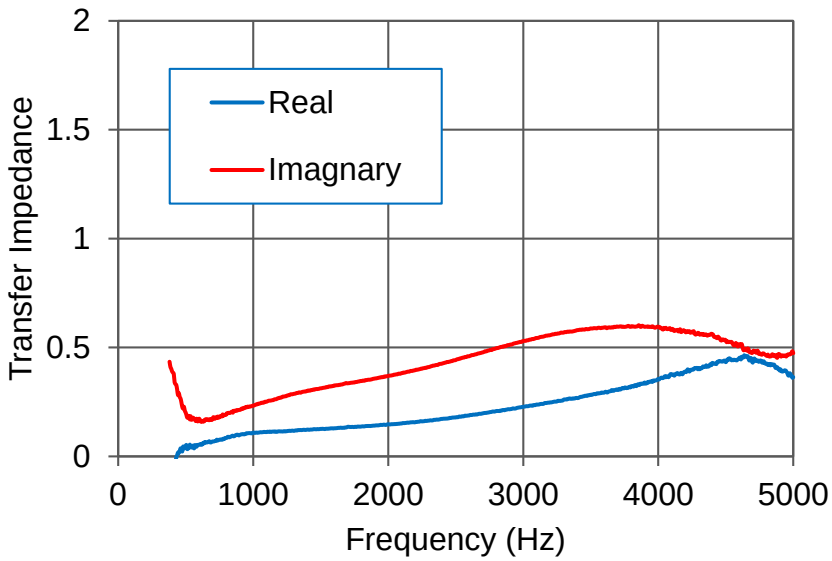

Figure 6.8 Transfer impedance of a perforated panel.

6.2.2 Sample Variation of Cover Transfer Impedance

The transfer impedance of 4 Samples of the cover shown in Figure 6.6a were measured using the procedure outlined in Section 5.3.1. Figures 6.10 and 6.11 show the real and imaginary parts of transfer impedance respectively for each of

the samples. Figure 6.12 shows the standard deviation for the 4 samples. There are noticeable differences between samples but the standard deviation is relatively low.

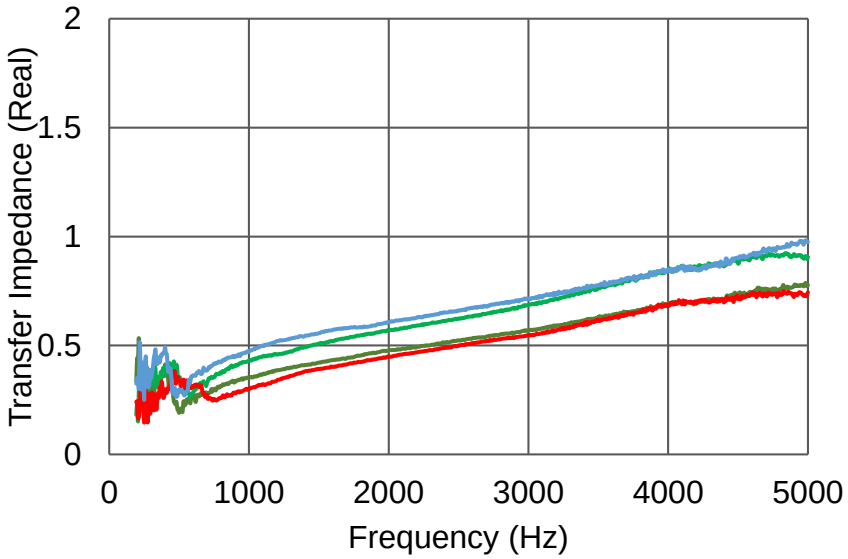

Figure 6.9 Variability of 4 samples of a cover (real part of transfer impedance).

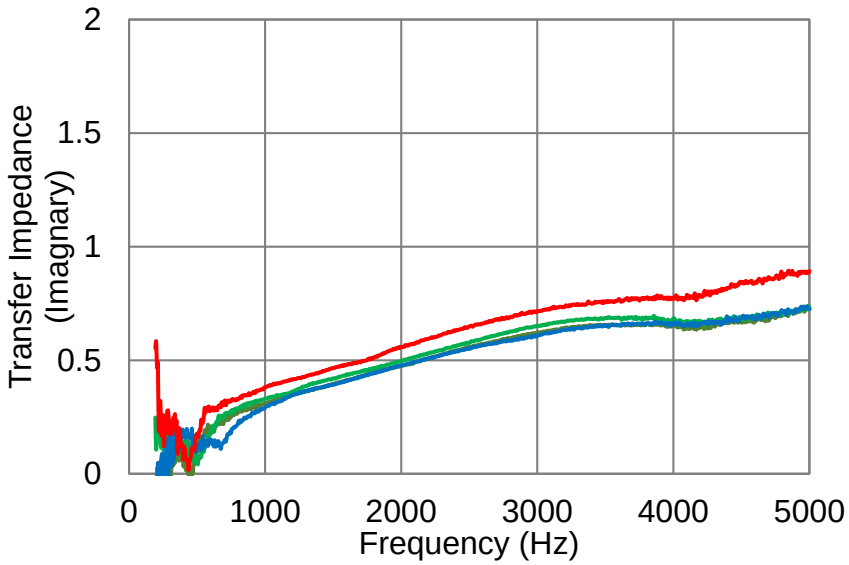

Figure 6.10 Variability of 4 samples of a cover (imaginary part of transfer impedance).

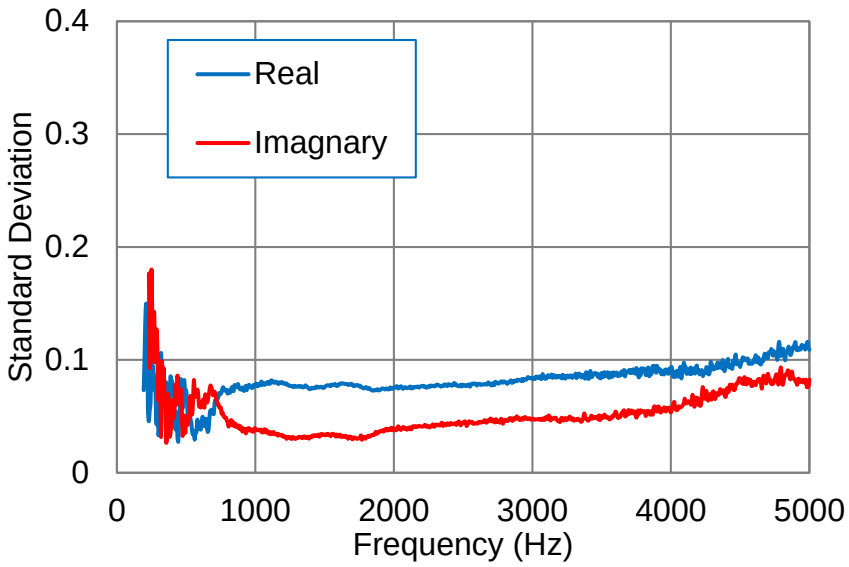

Figure 6.11 Standard deviation of transfer impedance for 4 samples of a cover.

6.3 Summary

The transfer impedance of increasing levels of glue was measured and compared in this chapter. Results show that both the real and imaginary parts of the transfer impedance increase with increasing levels of glue though the increase in the real part is less pronounced than the imaginary part of the transfer impedance. A similar amount of glue was applied to different substrates and compared. Results indicate that the transfer impedance can be quite different depending on the substrate. The transfer impedance of a fabric cover and a steel perforated panel were also measured using the impedance difference approach.

CHAPTER 7 SIMULATION OF BUILT-UP MATERIALS

7.1 Multi-Layer Material Test Case

The transfer matrix approach described in Section 5.3.2 was applied to layered materials. The built-up layered material is shown in Figures 7.1 and 7.2. The absorber consisted of a perforated cover, foam, and fiber. The cover was bonded to the foam and the foam and fiber were bonded together. The cover plus bonding was considered as a transfer impedance as was the bonding in between the foam and fiber. In this case, the bulk properties of the fiber and foam were measured using the three-microphone method introduced in chapter 3 and the transfer impedances of adhesive and top cover were measured using the impedance difference method introduced in chapter 5. After determining the properties of each layer, the transfer matrix approach which was introduced in Section 5.3.2 was used to predict the sound absorption and was then compared to the measured sound absorption.

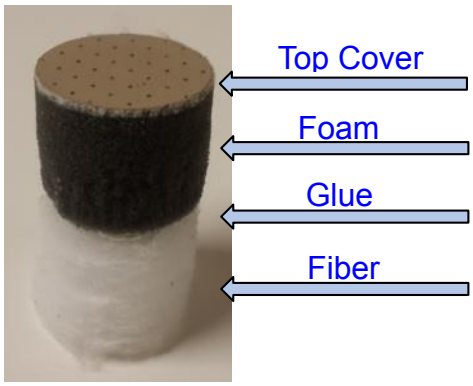

Figure 7.1 Composition of a multi-layer sound absorber.

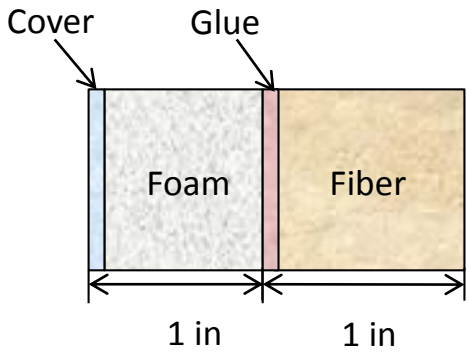

Figure 7.2 Schematic illustrating the composition of a multi-layer sound absorber.

The multi-layered material was separated in to two parts. The top cover with foam substrate was the first part and adhesive bonded with fiber was the second part. Each part was measured and compared with the transfer matrix method. The two parts were regrouped into the original lay-ups after achieving good agreement between measured and simulated results for each part.

The transfer impedance for the top cover is shown in Figure 7.3. Figure 7.4 shows the absorption coefficient of the top cover bonded with foam substrate. The transfer matrix method was compared to direct measurement result with good agreement.

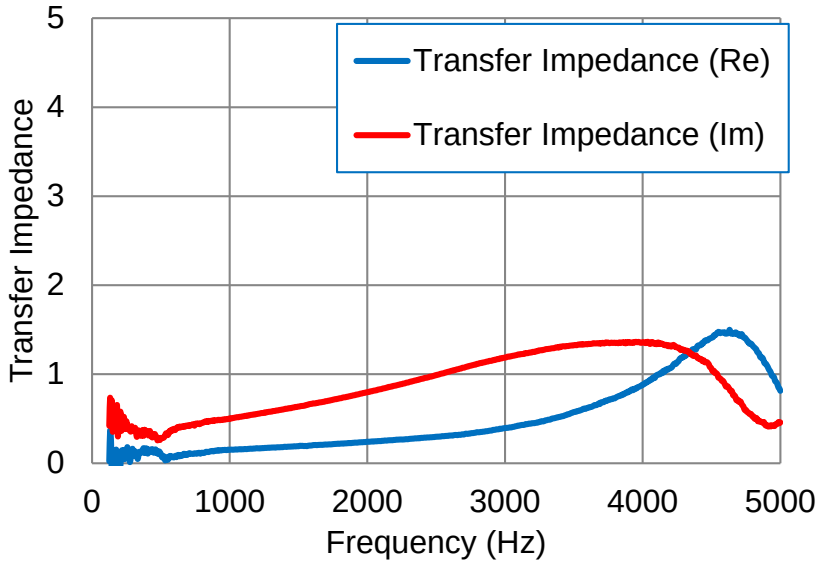

Figure 7.3 Transfer impedance of top cover.

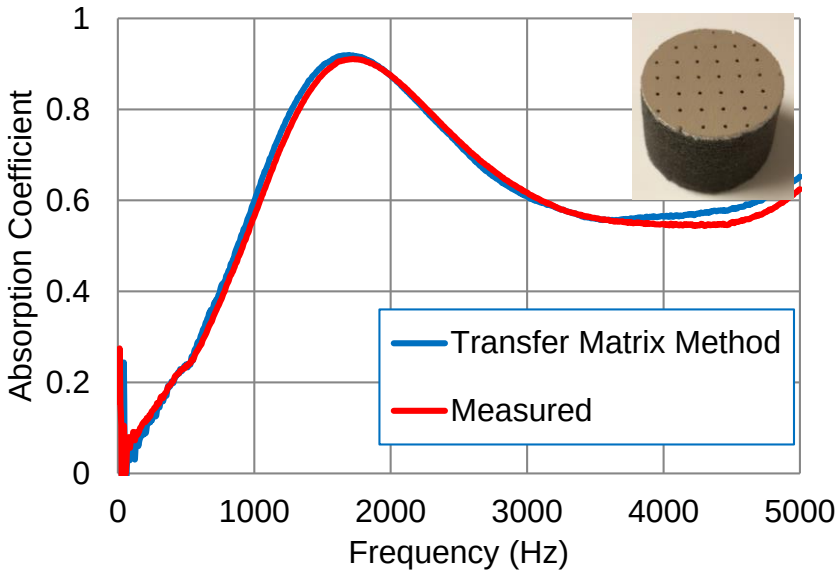

Figure 7.4 Sound absorption of top cover and foam substrate.

Figure 7.5 shows the transfer impedance of the adhesive determined via the impedance difference approach. Figure 7.6 shows the sound absorption of adhesive bonded with glass fiber. Both measurement and transfer matrix method compare very well, especially below 3000 Hz. There are some slight differences between the two methods above 3000 Hz.

After getting good agreement between measured and simulated results on each part, the two parts were then recombined to the original material lay-up. The sound absorption of the multi-layer sound absorber predicted by the transfer matrix method is compared to direct measurement in Figure 7.7 with good agreement up to 3000 Hz.

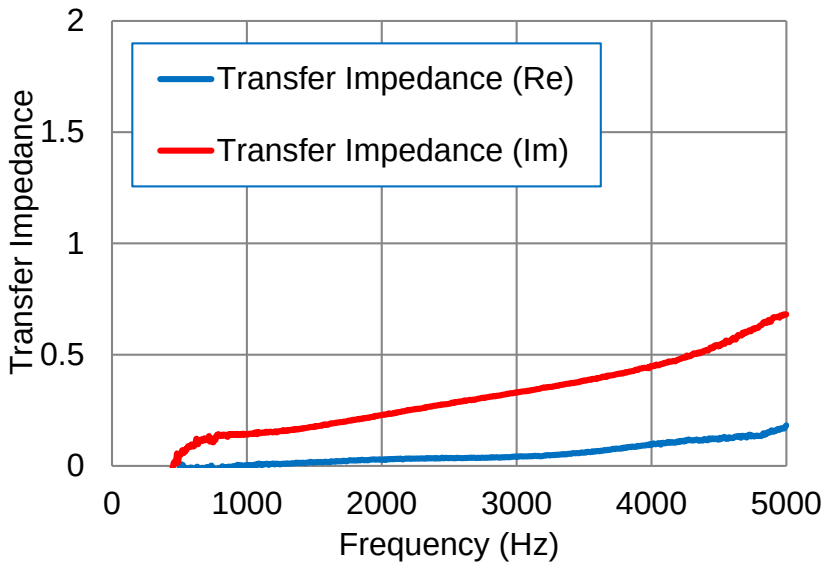

Figure 7.5 Transfer impedance of adhesive.

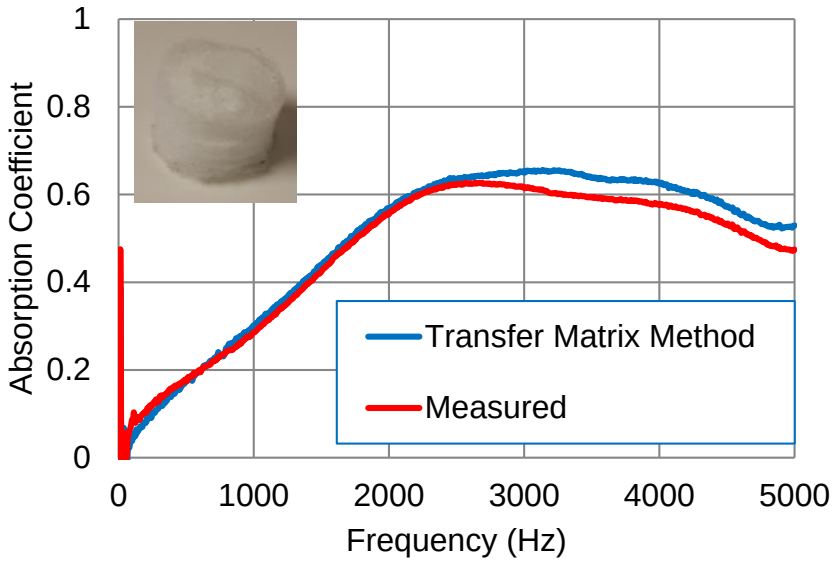

Figure 7.6 Sound absorption of adhesive bonded with glass fiber.

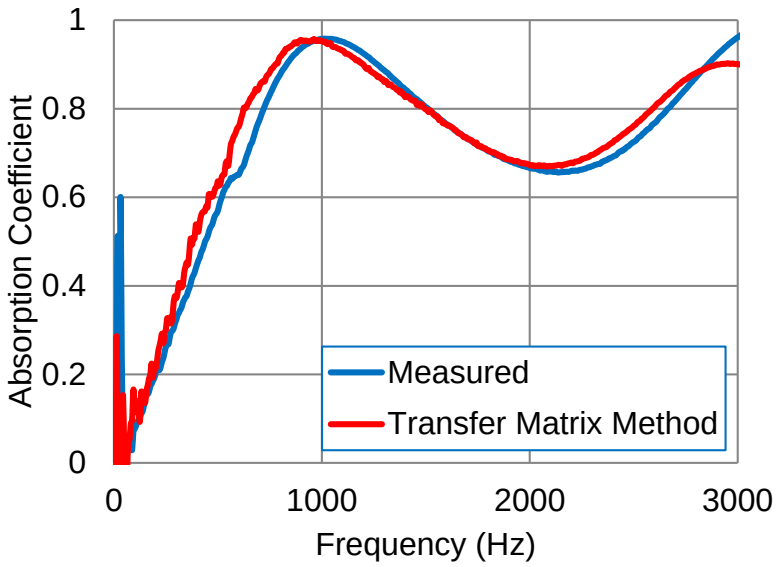

Figure 7.7 Sound absorption of a multi-layer sound absorber.

7.2 Summary

A procedure has been suggested in this chapter for the simulation of materials with covers and bonding materials. An impedance difference approach was used to determine the transfer impedance of the covers and bonding materials. The three-microphone approach was used to determine the characteristic impedance and complex wavenumber of the foam and fiber layers. After measuring the properties of the individual layers, the transfer matrix method was used to simulate the absorption of a layered absorber. The transfer matrix method was compared to measurement with good agreement. The suggested procedure would seem useful when simulating trim materials consisting of adhesives and densified covers.

CHAPTER 8 CONCLUSIONS AND RECOMMENDATIONS

8.1 Conclusions

The primary objective of this thesis was to determine the normal incident sound absorption coefficient of layered sound absorbers after determining the properties for the individual layers via measurement. The transfer matrix approach was used to calculate the sound absorption coefficient for the layered sound absorber. This thesis consists of four related investigations. In the first, the standard deviation of normal incident sound absorption impedance tube measurements was investigated. Secondly, several different methods for determining the acoustic properties of porous sound absorbing materials such as fibers and foams were compared to one another. In the third study, an impedance difference technique was proposed for determining the transfer impedance of adhesive layers, densified layers, and covers. After which, transfer matrix theory was used to simulate the acoustic performance of a layered sound absorber which consisted of layers of fiber and foam plus a cover and adhesive layer.

The effect of sample variation was investigated using 6 samples of melamine foam and 8 samples of glass fiber. Sample variation is mainly caused by 1) uneven thickness and density during material manufacturing, 2) sample size and shape, and 3) mounting the sample in the impedance tube. In order to minimize sample variation, considerable care was taken when preparing the sample for measurement. The sample was cut to fit snugly so that it was not compressed in the tube which can lead to shear resonances of the sample. Adding needles to samples was shown to be an effective method to eliminate shear resonances if the sample was slightly compressed. In addition, the cutting technique should be selected so that sample will not have an hourglass shape. Moreover, the use of a higher power sound source was shown to improve the measurement at low frequencies. After taking the precautions noted, it was shown that the standard deviations for the sound absorption coefficient of a melamine foam and glass

fiber were on average 0.03 and 0.02 respectively. It was also found that that the standard deviation could be as high as 0.07 for a slightly oversized sample.

The complex wavenumber and characteristic impedance are often used to characterize porous sound absorbers like foams and fibers. They are commonly referred to as bulk properties and are used for designing layered sound absorbers and can also be input into finite and boundary element models. In the second study, the many different measurement approaches for determining the bulk properties were surveyed. These approaches can be broken down into two classes; 1) direct and 2) indirect approaches.

The direct measurement approaches include the two load method (ASTM E2611), the two cavity method, and a newly developed three microphone method. The results demonstrated that all three approaches compared well though the three microphone method was demonstrated to produce the smoothest curve especially at low frequencies.

Three indirect methods were then examined. One approach is to measure the flow resistivity and then determine the bulk properties using an appropriate empirical equation. Alternatively, the sound absorption coefficient can be measured and then either the flow resistivity or the Biot properties can be determined using a least squares curve fit. The flow resistivity is curve fit using empirical equations while the Biot properties are determined based on an analytical model. It was shown that all three methods agreed well with one another. It was noted that measurement of the flow resistivity is the simplest and least expensive approach provided that the empirical equation is appropriate for a given material.

In the third study, the transfer impedance of covers and adhesives was determined using an impedance difference approach. The normal incident impedance of the sample was measured with and without the cover or adheive in place. The transfer impedance is the difference between the two measurements. Alternatively, the sample can be flipped and the difference between the two

measurements taken. The approach was validated by changing the thickness of the fiber or foam layer and insuring that the sound absorption could be predicted. The approach seems suitable as an engineering approximation in place of phenomenological models.

In the fourth study, the bulk properties and transfer impedance were integrated into a transfer matrix model of a multi-layer sound absorber. There was good agreement between the predicted and directly measured sound absorption coefficient for a multi-layer sound absorber consisting of a layer of foam, fiber, a cover, and an adhesive in between the fiber and foam layers. The good agreement demonstrates that the approaches can be used to determine the sound absorptive properties of layered sound absorbers.

8.2 Recommendations for Future Work

Based on the research in this thesis, the following recommendations can be made.

- Sample cutting and preparation is critical in order to obtain repeatable results in impedance tube measurements.
- The three-microphone method is recommended for directly measuring the bulk properties of fibrous or foam sound absorbers.
- The bulk properties can be indirectly predicted by measuring the flow resistivity. This approach, while approximate, is inexpensive and simpler than impedance tube measurements.
- An impedance difference approach can be used to determine the transfer impedance of an adhesive, perforate, cover, or densified layer.
- The aforementioned approaches could be used to determine the properties of individual layers and then combined to determine the sound absorption of a multi-layer sound absorber.

REFERENCES

J. Allard and N. Atalla, (2009). Propagation of Sound in Porous Media: Modelling Sound Absorbing Materials, 2nd Edition (Wiley, West Sussex, United Kingdom).

ASTM standard, (1998). "Standard Test Method for Using a Tube, Two Microphones and a Digital Frequency Analysis System," E1050-98.

ASTM standard, (2003). “Standard Test Method for Airflow Resistance of Acoustical Materials,” C522-03.

ASTM standard, (2009). “Standard Test Method for Measurement of Normal Incidence Sound Transmission of Acoustical Materials Based on the Transfer Matrix Method,” E2611-09.

T. Cox, and P. D’Antonio, (2004). Acoustic Absorbers and Diffusers: Theory, Design and Application (Spon Press, London).

M. E. Delany and W. A. Bazley, (1970). "Acoustical Properties of Fibrous Absorbent Materials," Applied Acoustics, 3, 105-116.

ESI Group, (2007). Foam-X User’s Guide.

X. Hua and D. W. Herrin, (2013). “Reducing the Uncertainty of Sound Absorption Measurements Using the Impedance Tube Method,” SAE Noise and Vibration Conference, Grand Rapids, MI, May 20-23, Paper No. 2013-01-1965.

T. Iwase, Y. Izumi, and R. Kawabata, (1998). “A New Measuring Method for Sound Propagation Constant by Using Sound Tube Without Any Air Spaces Back of a Test Materials,” Inter-Noise 98, New Zealand.

C. Jiang, T.W. Wu, C.Y.R. Cheng, (2010). “A single-domain boundary element method for packed silencers with mulriple bulk-reacting sound absorbing materials,” Engineering Analysis with Boundary Elements, vol. 34, pp. 971-976.

Naoki Kino and Takayasu Ueno, (2007). "Investigation of Sample Size Effects in Inpedance Tube Measurements," Applied Acoustics, 68, 1485-1493.

W. L. Li, X. Hua, and D. W. Herrin, (2014). “A Survey of Methods for Determining the Bulk Properties of Sound Absorbing Materials,” Proceedings of Noise-Con 2014.

F. P. Mechel, (1988). "Design Charts for Sound Absorber Layers," Journal of the Acoustical Society of America, 83, 1002-1013.

F. P. Mechel, (2008). Formulas of Acoustics, 2nd Edition (Springer Verlag, Berlin).

T. Melling, (1973). “The acoustic impedance of perforates at medium and high sound pressure levels,” Journal of Sound and Vibration, 29, 1–65.

M. L. Munjal, (1987). Acoustics of ducts and mufflers, Wiley, New York.

Office of Air Planning and Standards, (1995). “Glass Fiber Manufacturing”, Compilation of Air Pollutant Emission Factors, Volume 1: Stationary Point and Area Sources.

J. Pan and P. Jackson, (2009). “Review of Test Methods for Material Properties of Elastic Porous Materials,” *SAE Int. J. Mater. Manuf.* 2(1), 570-579.

M. Ren and F. Jacobsen, (1993). “A Method of Measuring the Dynamic Flow Resistance and Reactance of Porous Materials,” Applied Acoustics, 39, 265–276.

Y. Salissou and R. Panneton, (2010). “Wideband Characterization of the Complex Wave Number and Characteristic Impedance of Sound Absorbers,” Journal of the Acoustical Society of America, 128(5), 2868-2876.

A. F. Seybert, D. W. Herrin and X. Hua, (2013). "Controlling Uncertainty of Sound Absorption Measurements Using the Impedance Tube Method," Inter-Noise Conference, Innsbruck, Austria.

F. Simón, D. Fernandez, and J. Pfretzschner, (2006). "A Fitting method to Estimate the Air Flow Resistivity of Porous Materials," The Thirteenth International Congress on Sound and Vibration, Vienna, Austria.

B. H. Song and J. S. Bolton, (2001). “Effect of Circumferential Edge Constraint on the Acoustical Properties of Glass Fiber Materials,” Journal of the Acoustical Society of America, 110(6), 2902-2916.

Dan R. Stanley, (2012). "Impedance Tube Specimen Preparation and Mounting Issues," Inter-Noise Conference, New York, USA.

Z. Tao, D. W. Herrin and A. F. Seybert, (2003). “Measuring Bulk Properties of Sound-Absorbing Materials using the Two-Source Method,” SAE Noise and Vibration Conference and Exhibition, Traverse City, Michigan, USA, DOI. 2003-01-1586.

H. Utsuno, T. Tanaka, T. Fujikawa, and A. F. Seybert, (1989). "Transfer Function Method for Measuring Characteristic Impedance and Propagation Constant of Porous Materials," Journal of the Acoustical Society of America, 86(2), 637-643.

Q. Wu, (1988). "Empirical Relations between Acoustical Properties and Flow Resistivity of Porous Plastic Open-Cell Foam," Applied Acoustics, 25, 141-148.

T. W. Wu, C. Y. R. Cheng and Z. Tao, (2003). “Boundary Element Analysis of Packed Silencers with Protective Cloth and Embedded Thin Surfaces,” Journal of Sound and Vibration, 261, 1-15.

VITA

Wanlu Li was born in Jiangsu, China in 1987. She received Bachelor of Science degree in Mechanical Engineering from University of Kentucky in 2011. In August 2011, she enrolled in Department of Mechanical Engineering at University of Kentucky, for graduate study and research assistant. She had a Summer Internship job at Commercial Vehicle Group in 2013. During her graduate years at University of Kentucky, she published two Noise Control Engineering conference papers.